

RESEARCH ARTICLE

Targeting mitochondria in cancer therapy could provide a basis for the selective anti-cancer activity

Dmitri Rozanov^{1*}, Anton Cheltsov², Aaron Nilsen³, Christopher Boniface¹, Isaac Forquer⁴, James Korkola⁵, Joe Gray⁵, Jeffrey Tyner⁶, Cristina E. Tognon^{6,7,8}, Gordon B. Mills⁶, Paul Spellman¹

1 Department of Molecular and Medical Genetics, Knight Cancer Institute, Oregon Health and Science University, Portland, Oregon, United States of America, **2** Q-MOL LLC, San Diego, California, United States of America, **3** Medicinal Chemistry Core, Oregon Health and Science University, Portland, Oregon, United States of America, **4** Chemistry Department, Portland State University, Portland, Oregon, United States of America, **5** Department of Biomedical Engineering, Oregon Health and Science University, Portland, Oregon, United States of America, **6** Department of Cell, Developmental and Cancer Biology, Oregon Health and Science University, Portland, Oregon, United States of America, **7** Howard Hughes Medical Institute, Portland, Oregon, United States of America, **8** Division of Hematology & Medical Oncology, Oregon Health & Science University, Portland, Oregon, United States of America

* rozanov@ohsu.edu



OPEN ACCESS

Citation: Rozanov D, Cheltsov A, Nilsen A, Boniface C, Forquer I, Korkola J, et al. (2019) Targeting mitochondria in cancer therapy could provide a basis for the selective anti-cancer activity. PLoS ONE 14(3): e0205623. <https://doi.org/10.1371/journal.pone.0205623>

Editor: Aamir Ahmad, University of South Alabama Mitchell Cancer Institute, UNITED STATES

Received: September 25, 2018

Accepted: February 25, 2019

Published: March 25, 2019

Copyright: © 2019 Rozanov et al. This is an open access article distributed under the terms of the [Creative Commons Attribution License](https://creativecommons.org/licenses/by/4.0/), which permits unrestricted use, distribution, and reproduction in any medium, provided the original author and source are credited.

Data Availability Statement: All relevant data are within the manuscript and its Supporting Information files.

Funding: The authors received no specific funding for this work. The funder Q-MOL LLC provided support in the form of salaries for authors [AC], and has an additional role in the study in data collection and analysis and preparation of the manuscript. The specific roles of these authors are articulated in the 'author contributions' section.

Abstract

To determine the target of the recently identified lead compound NSC130362 that is responsible for its selective anti-cancer efficacy and safety in normal cells, structure-activity relationship (SAR) studies were conducted. First, NSC13062 was validated as a starting compound for the described SAR studies in a variety of cell-based viability assays. Then, a small library of 1,4-naphthoquinines (1,4-NQs) and quinoline-5,8-diones was tested in cell viability assays using pancreatic cancer MIA PaCa-2 cells and normal human hepatocytes. The obtained data allowed us to select a set of both non-toxic compounds that preferentially induced apoptosis in cancer cells and toxic compounds that induced apoptosis in both cancer and normal cells. Anti-cancer activity of the selected non-toxic compounds was confirmed in viability assays using breast cancer HCC1187 cells. Consequently, the two sets of compounds were tested in multiple cell-based and *in vitro* activity assays to identify key factors responsible for the observed activity. Inhibition of the mitochondrial electron transfer chain (ETC) is a key distinguishing activity between the non-toxic and toxic compounds. Finally, we developed a mathematical model that was able to distinguish these two sets of compounds. The development of this model supports our conclusion that appropriate quantitative SAR (QSAR) models have the potential to be employed to develop anti-cancer compounds with improved potency while maintaining non-toxicity to normal cells.

Introduction

Despite the advances achieved in the detection and treatment of early cancer that have contributed to declining cancer-specific mortality in the United States, metastatic cancer remains in

Competing interests: The authors have declared that no competing interests exist. Q-MOL LLC commercial affiliation does not alter our adherence to PLOS ONE policies on sharing data and material.

most cases an incurable disease. In this context, identifying new drugs and designing more efficacious and safe cancer treatments to prevent relapse in patients and to treat metastatic disease are clearly needed to provide an impact on cancer mortality rates.

One promising strategy for successful cancer therapy is to induce oxidative stress and followed by apoptosis in cancer cells but not in normal cells. Elevated levels of reactive oxygen species (ROS) and subsequent oxidative stress are hallmarks of carcinogenesis and metastasis providing a potential selective cytotoxicity index [1–3]. Our data and recent studies by others demonstrated that elevated levels of ROS can be exploited *in vitro* and *in vivo* to preferentially target cancer cells while sparing normal cells [4–7]. The ROS-based approach to induce apoptosis in cancer cells is conceptually different from conventional therapy targeting well known oncogenes and tumor suppressors—a therapy which is often ineffective due to multiple genetic and epigenetic alterations in cancer cells and the ability of cancer cells to upregulate compensatory mechanisms [8, 9]. The shortcomings of conventional targeted therapy approaches have prompted the development of alternative approaches. Instead of targeting specific oncogenes and tumor suppressors, exploiting common biochemical alterations in cancer cells, such as an increased ROS stress, could provide the basis for developing selective and potent therapeutic agents.

To cope with increased production of ROS, mammalian cells have developed two major electron donor systems, the thioredoxin (Trx) system and the glutathione (GSH) system [10, 11]. The Trx redox system is composed of thioredoxin reductase (TrxR), Trx, and NADPH while the GSH redox system is composed of GSR, GSH, and NADPH. The Trx and GSH system represent two complementary defense systems against oxidative stress. Other redox-sensitive enzymes that play a role in the oxidative stress response include Trx- and GSH-peroxidase, GSH-S-transferase (GST), and isocitrate dehydrogenase [12–14]. Thus, targeting any of these components can potentially induce oxidative stress which can result in cell death.

We recently reported the discovery of 1,4-naphthoquinone (1,4-NQ) derivative, NSC130362, which inhibits GSR and, as a consequence, induces oxidative stress and subsequent apoptosis in cancer cells but not in normal human primary hepatocytes. NSC130362 also showed anti-tumor activity *in vivo* [7]. In addition to inhibiting GSR, 1,4-NQs can be reduced by NADH/NADPH dehydrogenase followed by autoxidation, which results in the formation of ROS and potential oxidative stress. The extent of autoxidation is dependent on the type and position of substituents. 1,4-NQs can also reduce cell viability *via* arylation of cellular nucleophiles such as GSH, DNA, RNA and proteins and also by inhibition of DNA synthesis or mitochondrial function [15–17]. In the current work, we tested different activities of NSC130362 and its analogs with the aim of identifying the factors responsible for enabling NSC130362's selective anti-tumor activity. Based on the obtained results, we were able to construct a mathematical model that could distinguish toxic NSC130362 analogs from analogs that were non-toxic to normal cells.

Materials and methods

Reagents

All reagents were from Sigma, unless otherwise indicated. CellTiter-Glo reagent was from Promega. Glutathione reductase (GSR) activity kit was from Cayman. GSR producing plasmid was a kind gift of Dr. Becker (Justus-Liebig University Giessen). GSR was expressed in BL21 (DE3) cells and purified by both metal chelating and affinity chromatography on 2',5'-ADP-Sepharose as described [18].

Cells

Human prostate carcinoma, breast, and pancreatic carcinoma cells were obtained from ATCC. Chemotherapy resistant prostate carcinoma cells were from Dr. Korkola. Human

primary hepatocytes were obtained from Lonza. All cells were cultured according to the provider's guidelines. Bone marrow aspirates or peripheral blood samples were collected from acute myeloid leukemia (AML) patients under an OHSU Institutional Review Board (IRB) approved research collection protocol which covers *in vitro* drug testing of leukemia cells and genetic studies. Patients signed an IRB-approved written consent form after verbal consent was obtained. Mononuclear cells were isolated from peripheral blood samples using a Ficoll gradient and viability of isolated mononuclear cells was assayed using Guava Viacount reagent. All patients were treated in accordance with the ethical guidelines laid out in the Declaration of Helsinki. AML cells were cultured in RPMI medium supplemented with 10% fetal bovine serum.

Hydrogen peroxide cell-based assay kit

Cells were incubated for 2 h with either compounds (30 μM) or DMSO in a 96-well plate. After the treatment, 80 μl of cell culture medium was collected and the level of hydrogen peroxide was determined using a Hydrogen Peroxide Cell-Based Assay kit (Cayman).

Glutathione reductase (GSR) activity assay

Recombinant GSR (0.5 u/well) in a 96-well plate was incubated in the GSR assay buffer (50 mM potassium phosphate buffer, pH 7.5 supplemented with 1 mM EDTA), 100 μl with and without compound (30 μM) for 2 h at 25°C. At the end of incubation, 100 μl of solution containing NADPH (0.087 mM), oxidized glutathione (GSSG) (0.95 mM) and 1 μl of the reagent that detects ratio of GSSG to reduced glutathione (GSH) (Abcam) were added and the mixture was incubated for an additional 1 h at 25°C. GSR activity was measured by using 490-nm excitation and monitoring fluorescence at 520 nm with a fluorescence plate reader. One unit of GSR activity was defined as the amount of enzyme required to produce 1 μM of GSH in a total reaction volume of 200 μl in 1 minute in the GSR assay buffer containing NADPH (0.087 mM), GSSG (0.95 mM) and 1 μl of GSH/GSSG ratio detection reagent (Abcam).

NADH/NADPH dehydrogenase-mediated ROS generation assay

Recombinant NADH/NADPH dehydrogenase (0.5 units/well) in a 96-well plate was incubated in 100 μl of the assay buffer (50 mM potassium phosphate buffer, pH 7.5 supplemented with 1 mM EDTA) containing NADPH (3 μM) and superoxide dismutase (SOD) (100 units/well) with and without compound (30 μM) for 4 h at 37°C. At the end of incubation, the level of hydrogen peroxide was measured using a Hydrogen Peroxide Assay kit (Cayman). Control samples were without NADH/NADPH dehydrogenase. The rate of NADH/NADPH dehydrogenase- and compound-mediated ROS production was determined by subtracting values that were obtained in the absence of NADPH dehydrogenase. One unit of NADH/NADPH dehydrogenase was defined as the amount of enzyme required to reduce 1.0 μmole cytochrome C per min/mg in the presence of menadione substrate at 37°C. One unit of SOD was defined as the amount of enzyme required to inhibit reduction of cytochrome C by 50% in a coupled system with xanthine oxidase at pH 7.8 at 25°C in a 3.0 mL reaction volume. Xanthine oxidase concentration should produce an initial ΔA_{550} of 0.025 ± 0.005 per min.

MitoCheck Complex I activity assay

MitoCheck Complex I activity was determined as described in the manual of the manufacturer's manual (Cayman). Briefly, compounds (30 μM) or DMSO were mixed with the Complex I activity assay buffer that contained bovine heart mitochondria reagent, NADH, and

ubiquinone in the presence of KCN to inhibit complex IV activity. The level of Complex I activity was monitored in a kinetic assay of NADH oxidation by measuring a decrease in absorbance at 340 nm. The residual Complex I activity was calculated by dividing the rate of compound wells by the rate of DMSO wells for the linear portion of the curve.

Glyceraldehyde-3-phosphate dehydrogenase (GAPDH) activity assay

Cells were incubated for 2 h with either compounds (30 μ M) or DMSO in a 6-well plate. Next, cells were collected in 200 μ l of PBS and disrupted by sonication. Insoluble material was removed by centrifugation. The level of GAPDH activity was determined by GAPDH activity assay kit (BioVision).

Small-molecule compounds

NSC130362 and its analogs were obtained from the NCI/DTP Open Chemical Repository (<http://dtp.nci.nih.gov/repositories.html>). Clinical drugs were purchased as dry powders from Cayman.

Statistical analysis

The results of the different assays are expressed as mean values based on at least three replicates. The statistical significance of differences in the treatment outcomes was determined by one-way ANOVA or t-tests.

Results

Characterization of NSC130362 as a lead compound

The NIH has defined several requirements that should be met for a compound to be considered as a starting material for drug discovery programs [19]. Starting compounds should (1) elicit a reproducible response in at least two assay types and have a dose-response over a hundred-fold concentration range; (2) be analytically validated in terms of integrity and purity; (3) demonstrate adequate potency; (4) possess a tractable starting point of chemical optimization with no obvious major chemical liabilities. Most of these requirements were addressed in our previous publication [7]. Thus, we demonstrated that our lead compound, NSC130362 (Fig 1A) selectively induces reproducible responses in either oxidative stress or caspase 3/7 activity assays in cancer cells. We also showed that its combination with different oxidative stress inducers, such as arsenic trioxide (ATO), myricetin (Myr), and buthionine sulfoximine (BSO), caused cell death in a variety of breast, pancreatic, prostate, and lung carcinoma cell lines as well as in human melanoma MDA-MB-435 and AML cells from patients. Finally, NSC130362 demonstrated anti-tumor activity *in vivo* [7]. To complement these results, we performed dose-response studies in pancreatic carcinoma MIA PaCa-2 cells (Fig 1B). The obtained data clearly showed that NSC130362 induced a dose-response over a hundred-fold concentration range in the presence of ATO. In addition, the structure of NSC130362 was verified *via* proton NMR and compound purity was at least 97% as determined by HPLC with UV detection at 280 nm. According to the structure, this compound can be easily modified to produce chemically related analogs [20].

NSC130362 is a 1,4-NQ. Quinone moieties are present in many drugs such as anthracyclines, daunorubicin, doxorubicin, mitomycin, and saintopin, which are used in anti-cancer therapy [15]. The effects of quinones on cell viability are mainly due to generation of reactive oxygen species (ROS) or to covalent attachment to biomolecules *via* arylation reactions [15, 21]. In addition to their ability to induce oxidative stress, ROS-generating agents can also

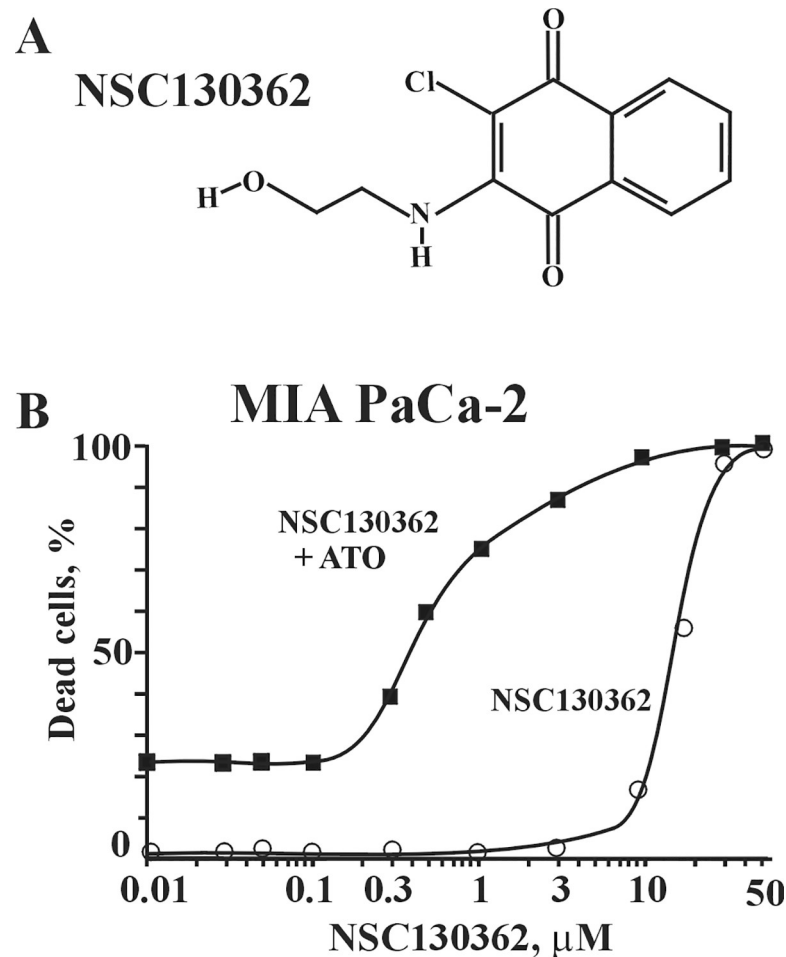


Fig 1. A, Structure of NSC130362. B, Dose response curve of NSC130362 in MIA PaCa-2 cells. Cells were pre-incubated with NSC130362 for 2 h followed by addition of ATO (5 μM) and incubation for an additional 24 h. At the end of the treatment, the ratio of dead cells was determined by a CellTiterGlo reagent. $P < 0.05$.

<https://doi.org/10.1371/journal.pone.0205623.g001>

potentiate the ability of clinical drugs to induce apoptosis in cancer cells [22–24]. To test whether NSC130362 is able to promote the cytotoxic effect of anti-cancer drugs, we performed cell viability assays using chemotherapy resistant PANC1 and YAPC pancreatic carcinoma cells (Fig 2). We found that NSC130362 significantly increased the ability of all tested pancreatic cancer drugs [25] to induce apoptosis in PANC1 and YAPC cell lines. To further validate these findings, we analyzed a variety of chemotherapy resistant prostate carcinoma cells in cell viability assays using prostate cancer drugs docetaxel and enzalutamide (MDV3100) either alone or in combination with NSC130362 (Fig 3). For comparison purposes, we also included FDA-approved ATO in this analysis. Our selection of ATO was based on our previous findings showing that ATO and NSC130362 exhibited synergistic responses against multiple cancer cells [7]. As we expected, NSC130362 efficiently potentiated the effect on cell viability of either ATO or MDV3100. NSC130362 also potentiated docetaxel-induced cytotoxicity, but to a lesser extent most likely because docetaxel was more cytotoxic as monotherapy than MDV3100 and ATO. Finally, we performed screening of small-molecule kinase inhibitor libraries [26] with and without NSC130362 against freshly isolated primary acute myeloid leukemia (AML) cells obtained from patients. Encouragingly, NSC130362 decreased EC50 (cytotoxicity) of several

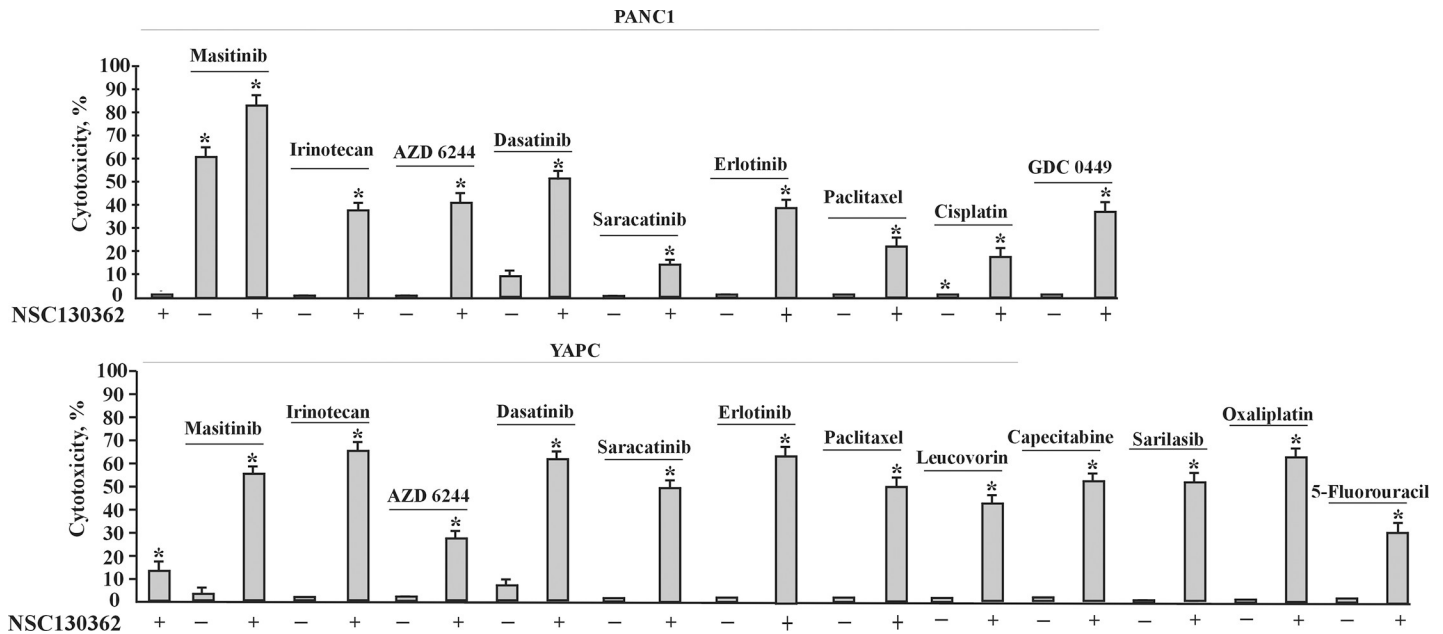


Fig 2. Combined treatment of NSC130362 with pancreatic cancer drugs against PANC1 and YAPC cells. Cells were pre-incubated with NSC130362 (10 μM) for 2 h followed by addition of drugs (10 μM) and incubation for an additional 24 h. At the end of the treatment, the ratio of dead cells was determined by a CellTiterGlo reagent. The first bar is NSC130362 alone. *, $P < 0.05$.

<https://doi.org/10.1371/journal.pone.0205623.g002>

kinase inhibitors by 1000-fold (Supporting Information S1 Table). We also found that there were a number of shared kinase inhibitors across leukemia cells from three different patients whose activity was significantly induced (more than 10 times) by NSC130362. In summary, in

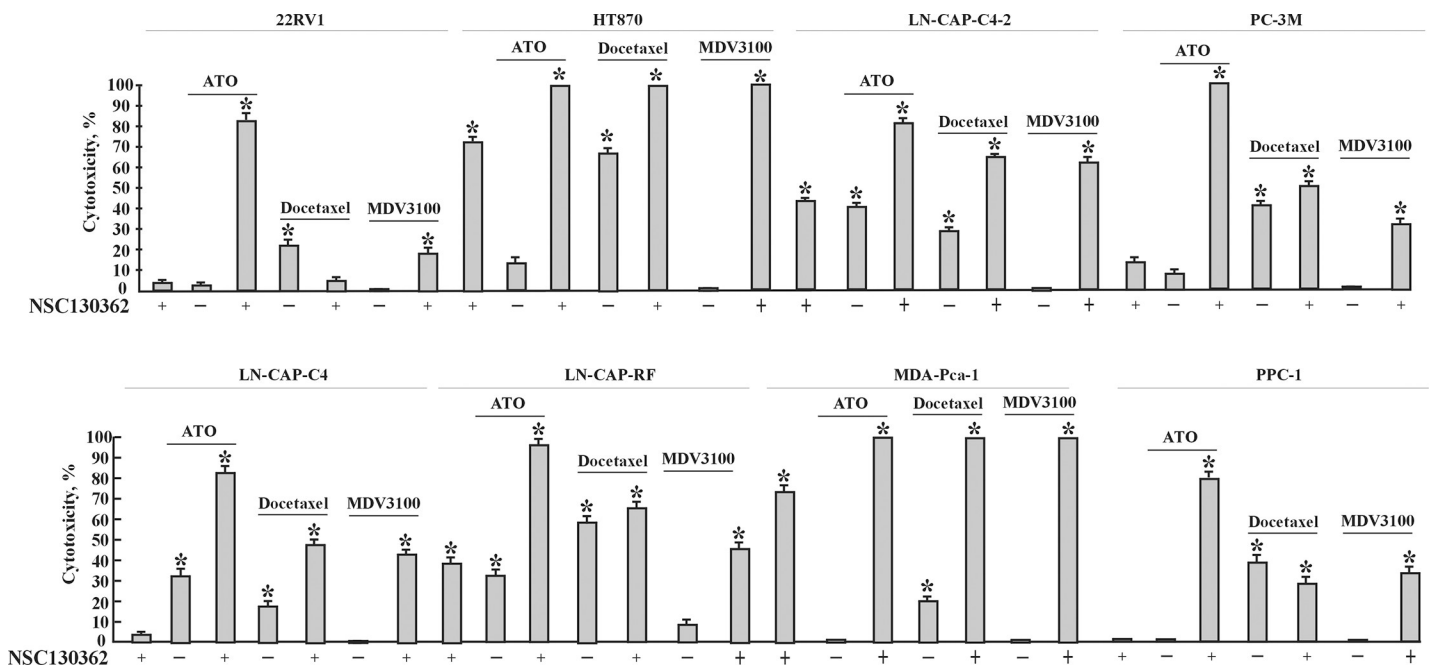


Fig 3. Combined treatment of NSC130362 with ATO, docetaxel, and MDV3100 against prostate cancer cells. Cells were pre-incubated with NSC130362 (10 μM) for 2 h followed by addition of drugs (10 μM) and incubation for an additional 24 h. At the end of the treatment, the ratio of dead cells was determined by a CellTiterGlo reagent. The first bar in the treatment of each cell line is NSC130362 alone. *, $P < 0.05$.

<https://doi.org/10.1371/journal.pone.0205623.g003>

these independent analyses, NSC130362 exhibited synergistic anti-tumor activity against different cancer cell types when combined with distinct FDA-approved drugs and kinase inhibitors. Based on these findings, we conclude that NSC130362 is a promising starting compound for further characterization.

Mechanisms underlying NSC130362-mediated effects in cancer cells

To elucidate the mechanism of synergy between NSC130362 and ATO, we analyzed the effect of a reducing environment on cytotoxic activity mediated by the NSC130362/ATO combination. The rationale for this assay was based on the knowledge that NSC130362, in addition to its ability to induce ROS *via* NADH/NADPH dehydrogenase-mediated reaction, targets GSR, an enzyme that maintains the reducing environment of the cell and is critical in resisting oxidative stress. In turn, ATO interferes with numerous intracellular signal transduction pathways that may result in the induction of apoptosis, the inhibition of tumor growth, and angiogenesis [27]. These effects, at least in part, are mediated *via* interaction of ATO with redox-sensitive proteins and enzymes. Almost all ATO-interacting proteins are protected against oxidation by the highly reduced intracellular environment that is controlled by GSR. Thus, GSR inhibition could facilitate ATO-mediated oxidation of intracellular proteins resulting in a synergistic induction of apoptosis in cancer cells. In agreement, our data showed that the effect of NSC130362/ATO combination is inhibited by dithiothreitol (DTT) (Fig 4). Thus, we conclude that the effect of NSC130362 on ATO-mediated cytotoxicity is mediated, at least in part, by its ability to induce ROS and/or inhibit GSR. We also tested the effect of hypoxic conditions on the activity of NSC130362/ATO combination. The effect of low level of oxygen on NSC130362/ATO-mediated cytotoxicity in MIA PaCa-2 cells was less pronounced than that of DTT (Fig 4).

Structure-activity relationship studies of NSC130362 analogs

To evaluate the effect of substituents on the cytotoxic activity of NSC130362 analogs toward cancer and normal cells, we analyzed cell viability after treatment with compounds in the

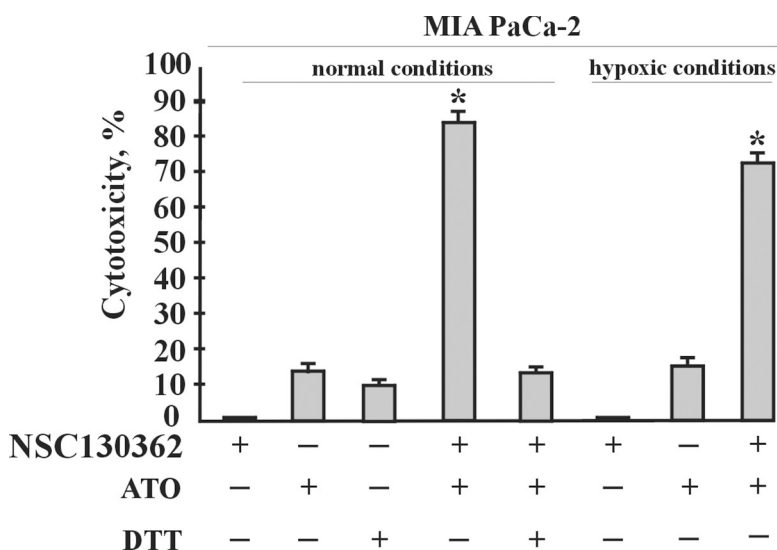


Fig 4. Effect of DTT and hypoxic conditions on the activity of NSC130362/ATO combination in MIA PaCa-2 cells. Cells were pre-incubated with NSC130362 (3 μM) in either normal (24% O₂) or hypoxic (0.5% O₂) conditions for 2 h in the presence or absence of DTT (3 mM) followed by addition of ATO (5 μM) and incubation for an additional 24 h. At the end of the treatment, the ratio of dead cells was determined by a CellTiterGlo reagent. *P*<0.05.

<https://doi.org/10.1371/journal.pone.0205623.g004>

absence or presence of ATO using pancreatic cancer MIA PaCa-2 cells and human primary hepatocytes. We selected MIA PaCa-2 cells because these cells are highly responsive to ROS [7]. These cells were also selected because of their robust engraftment in immunodeficient mice and sensitivity to ROS-inducing agents *in vivo*. Importantly, the results obtained in MIA PaCa-2 cells are similar to those obtained in breast and other cancer cells [7]. We selected hepatocytes as normal cells because hepatocytes are mediate toxicity to multiple drugs and are used as a standard to assess toxicity of drugs *in vitro* [28]. We then determined the selective cytotoxicity index of each NSC130362 analog by dividing the EC50 (cytotoxicity) measured in hepatocytes by that obtained in cancer cells in the presence of ATO. Because ATO and NSC130362 showed clear synergy against MIA PaCa-2 cells (Fig 1) [7], the selective cytotoxicity index was related to the combined treatment, however, data for monotherapy were also provided. ATO at the concentration of 5 μ M did not affect the viability of both MIA PaCa-2 cells and human hepatocytes. For comparison with the standard of care, doxorubicin was also included in this analysis. In addition to its effect on DNA replication, doxorubicin is also known as an oxidative stress inducer [29].

We performed SAR studies to understand the chemical–biological interaction controlling cytotoxicity in MIA PaCa-2 cells without affecting the viability of human hepatocytes. To cover more chemical space, in addition to 1,4-NQs, quinoline-5,8-diones were also analyzed (Fig 5).

First, we analyzed 2-chloro-3-amino-1,4-NQ and 2-chloro-3-(alkylamino)-1,4-NQs (Fig 6). SAR results showed that the cytotoxic activity of compounds 1–9 in cancer cells depends on the size of the 3-substituent. The anti-cancer potency and selective cytotoxicity index decreased with increased length of the substituent. When compounds with branched 3-(alkylamino) substituent (compounds 10–13) were analyzed, we also noticed a decrease in cytotoxic activity and selective cytotoxicity index when the length of alkyl chain is changed from isopropyl (compounds 10) to either sec-butyl or isobutyl (compounds 11 and 12, respectively). However, when the alkyl group was tert-butyl (compounds 13) there was a significant increase in the anti-cancer activity and selective cytotoxicity index. We conclude that the shape of 4-carbon alkyl group plays an important role in the biological activity of the analyzed compounds. The importance of the shape of the alkyl substituent in 2-chloro-3-(alkylamino)-1,4-NQs can be drawn from study of compounds 14–16. In this case, when two hydrogens of the amino group are substituted by either two methyl groups (compound 14) or aziridine groups (compound 15), the resulting compounds have similar cytotoxic activity in MIA PaCa-2 cells to a compound when one hydrogen of the amino group is substituted by the methyl group

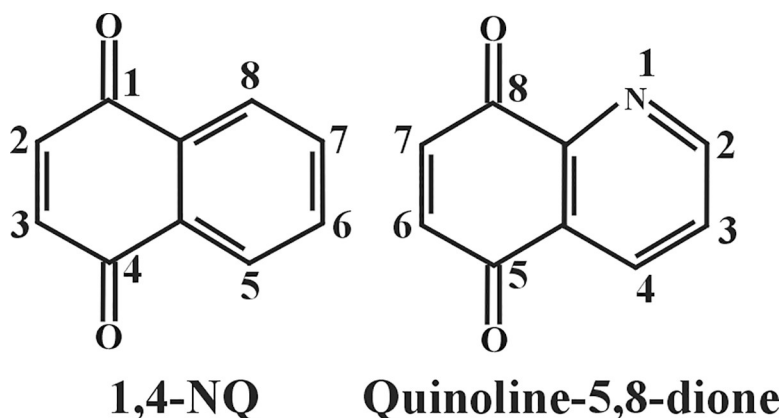


Fig 5. Structure of 1,4-NQ and quinoline-5,8-dione.

<https://doi.org/10.1371/journal.pone.0205623.g005>

N	Name	Structure	EC50, μ M				Selective cytotoxicity index	N	Name	Structure	EC50, μ M				Selective cytotoxicity index	N	Name	Structure	EC50, μ M				Selective cytotoxicity index
			MIA PaCa-2		Hepatocytes						MIA PaCa-2		Hepatocytes						MIA PaCa-2		Hepatocytes		
			ATO	ATO	ATO	ATO					ATO	ATO	ATO	ATO					ATO	ATO	ATO	ATO	
1	NSC9310		8.4	0.2	17.0	19.1	95.5	17	NSC130362		9.8	1.8	83.0	70.0	38.9	33	NSC130440		7.9	1.8	25.4	10.5	5.8
2	NSC91104		38.6	1.4	41.1	19.3	13.8	18	NSC93944		27.5	2.2	75.3	22.9	10.4	34	NSC41101		18.1	6.4	11.8	7.7	1.2
3	NSC3860		59.0	2.9	81.9	74.0	25.5	19	NSC296646		24.9	53.3	47.8	51.5	1.0	35	NSC22338		8.0	0.8	11.5	7.0	8.8
4	NSC91105		90.0	9.7	90.0	89.4	9.2	20	NSC22705		>90.0	53.3	47.8	51.5	1.0	36	NSC41098		16.2	8.4	8.8	6.4	0.8
5	NSC91106		>90.0	20.4	>90.0	>90.0	4.4	21	NSC91098		13.8	0.9	60.4	23.0	25.6	37	NSC40344		5.2	0.9	6.0	6.3	7.0
6	NSC91110		>90.0	20.1	>90.0	>90.0	4.5	22	NSC93948		39.0	3.4	90.0	29.4	8.6	38	NSC337757		>90.0	>90.0	26.0	24.0	0.3
7	NSC130320		26.1	21.0	>90.0	>90.0	4.3	23	NSC91099		27.7	1.6	85.7	62.2	38.9	39	NSC4285		3.9	1.6	2.3	1.2	0.8
8	NSC91101		>90.0	62.8	78.6	54.6	0.9	24	NSC91100		55.4	2.6	67.8	26.0	10.0	40	NSC142581		78.5	21.3	24.5	19.6	0.9
9	NSC91109		>90.0	80.6	>90.0	84.9	1.1	25	NSC93950		82.1	8.6	60.8	28.7	3.3	41	NSC102396		2.5	1.2	8.4	7.9	6.6
10	NSC91102		69.0	4.0	>90.0	51.3	12.8	26	NSC106715		26.6	13.7	4.8	3.6	0.3	42	NSC130385		3.2	1.3	10.0	2.5	1.9
11	NSC91103		>90.0	12.0	>90.0	>90.0	7.5	27	NSC93949		0.9	0.9	24.1	9.7	10.8	43	NSC102397		>90.0	22.7	>90.0	>90.0	4.0
12	NSC91108		>90.0	13.1	>90.0	>90.0	6.9	28	NSC91760		9.2	2.1	48.5	30.0	14.3	44	NSC202632		7.0	2.6	5.3	2.9	1.1
13	NSC91107		7.2	1.0	29.9	26.8	26.8	29	NSC4264		5.4	0.9	9.7	8.1	9.0	45	NSC92080		2.5	0.6	2.6	0.7	1.2
14	NSC7		7.2	1.8	10.0	9.3	5.2	30	NSC124993		5.7	4.7	3.6	5.8	1.2	46	NSC240656		5.2	1.6	2.9	4.6	2.9
15	NSC35851		2.3	1.2	2.6	2.9	2.4	31	NSC124994		10.4	5.9	1.6	1.3	0.2	47	NSC106442		7.0	3.9	9.0	7.4	1.9
16	NSC35852		6.9	1.0	78.0	>90.0	90.0	32	NSC130441		10.2	6.7	2.2	1.6	0.2		Doxorubicin		0.7	0.2	10.0	0.7	3.5

Fig 6. EC50 values and the selective cytotoxicity index of the NSC130362 analogs that contain 3-chloro substituent in MIA PaCa-2 cells and hepatocytes. Doxorubicin was included as a reference compound. Standard deviation for all EC50 values does not exceed 10%. To calculate the selective cytotoxicity index for compounds that have the EC50 value above 90 μ M, EC50 values were equated to 90 μ M. $P < 0.05$.

<https://doi.org/10.1371/journal.pone.0205623.g006>

(compound 2). However, the effect of these substitutions on toxicity to hepatocytes was more pronounced. Compounds 14 and 15 were approximately 2 and 6.5 times more toxic toward hepatocytes than compound 2, respectively. Strikingly, when two methyl groups were attached to the aziridine group (compound 16), the compound became completely non-toxic against normal cells, while maintaining almost identical levels of anti-cancer activity with that of compound 15. These data showed again that the shape of the 3-substituent is an important factor, which is responsible for the compound's biological activity. Unfortunately, the steric contribution of the 3-position substituents is difficult to predict due to the absence of data regarding target protein/compound interactions.

Next, we analyzed different 2-chloro-3-(hydroxylalkylamino)-1,4-NQs where the alkyl group contains single hydroxyl groups (compounds 17–19). In contrast to compounds 3 and 4, change of the 2-hydroxyethyl group (compound 17) for either 3-hydroxypropyl (compound

18) or 2-hydroxypropyl (compound **19**) had little effect on the anti-cancer activity but increased toxicity to hepatocytes approximately 3-fold. In compounds **3** and **4**, changing of the ethyl group for the propyl group had little effect on toxicity to hepatocytes but reduced anti-cancer activity more than 3-fold. On the other hand, exchange of the ethyl group in compound **3** for the isopropyl group (compound **10**), had little effect on activity against cancer cells or hepatocytes. We conclude again that shape of the alkyl chain in the 3-position contributes to the biological activities of the compounds. To analyze the effect of hydroxyl substitution in the alkyl group, we compared compounds **3** vs **17**, and **4** vs **18** vs **19**. While, compounds **3** and **17** had similar anti-cancer activity and toxicity towards hepatocytes, addition of a hydroxyl group to the propyl group to generate 3-hydroxypropylamino (compound **18**) and 2-hydroxypropylamino (compound **19**) substituent resulted in approximately 2- and 4-fold increase in anti-cancer activity and toxicity to hepatocytes, respectively. We conclude that the hydroxyl group non-specifically increases cytotoxic activity of compounds **18** and **19**. In contrast, addition of 3 hydroxyl groups to the tert-butylamino substituent of compound **13** to generate compound **20**, resulted in approximately 50- and 2-fold loss in anti-cancer activity and toxicity to hepatocytes, respectively. These data suggest that the effect of hydroxyl group in the 3-alkylamino substituent is variable and depends on the length and shape of the alkyl chain.

We also analyzed the effect of different alkoxyamino substituents on biological activity of 2-chloro-3-(alkoxyamino)-1,4-NQs (compounds **21**–**26**). As in the case with compounds **3** and **4**, change of the 2-methoxyethylamino substituent (compound **21**) for 3-methoxypropylamino group (compound **22**) resulted in a 4-fold decrease in anti-cancer activity with little effect on toxicity to hepatocytes. However, the effect of attachment of a methoxy group to the C-2 position of the propylamino substituent (compound **23**) on anti-cancer activity is less pronounced with a decrease in toxicity to hepatocytes of almost 3-fold. These data again point to the significance of steric effects of the 3-position substituents in 2-chloro-3-(alkoxyamino)-1,4-NQs. A similar trend in decreased anti-cancer activity with increasing the length of 3-substituent was seen when the 2-methoxyethylamino substituent in compound **21** was changed for the 2-ethoxyethylamino (compound **24**), the 3-isopropoxypropyl (compound **25**) or the 3-butoxypropylamino group (compound **26**). However, while compounds **21**, **24**, and **25** have similar toxicity to hepatocytes ($EC_{50} = 23$ – 29), the presence of 3-butoxypropylamino substituent in compound **26** drastically increased toxicity to hepatocytes ($EC_{50} = 3.6$). The positive effect of a methoxy group on the anti-cancer activity was seen by comparing compounds **3** vs **21**, and **4** vs **22** but the presence of a methoxy group also increased toxicity to hepatocytes approximately 3-fold. In contrast, attachment of a methoxy group at the C-2 position of 3-propylamino substituent (compound **23**) resulted in a 6-fold improved anti-cancer activity without significant effect on toxicity to hepatocytes as compared to compound **4**. By comparing compounds **21** vs **24**, and **22** vs **25** vs **26**, it was evident that increasing the length of alkoxy attachment to the 3-alkylamino substituent decreased anti-cancer activity and can, as in the case of compound **26**, increase toxicity to hepatocytes. We conclude that because the alkoxy group can have different effects on anti-cancer activity and toxicity to hepatocytes (compare compounds **4** vs **22** and **4** vs **23**), it is possible, *via* careful selection of the C-3 position substituent, to improve anti-cancer potency while maintaining low toxicity to hepatocytes. A 10.8-fold improvement in the anti-cancer activity of compound **4** was seen when the 3-propylamino substituent was extended by the dimethylamino group (compound **27**), however, it also increased toxicity to hepatocytes 9.2 times. When the 3-propylamino substituent of compound **4** was extended by the bis(2-hydroxyethyl)amino moiety (compound **28**), anti-cancer activity and toxicity to hepatocytes were increased 4.6- and 3.0-fold, respectively.

Both, the presence of carbonyl group and increasing the length of the C-3 position substituent were unfavorable in relation to the development goals as was evidenced by gradual

decrease in the anti-cancer activity and an increase in the toxicity to hepatocytes of compounds **29**, **30**, **31**, and **32** as compared to compound **1**. Substitution of hydrogen with a chloro group in the 3-acethylamnio substituent of compound **29** to generate compound **33**, caused 2-fold decrease in the anti-cancer activity. Extension of the C-3 position amino substituent in compound **1** by either the 2-oxo-2-hydroxyethyl (compound **34**) or the 2,2,2-trifluoroacetamide group (compound **35**) also decreased the anti-cancer activity and increased toxicity to hepatocytes. We conclude that in all cases the presence of a carbonyl group in the C-3 position substituent made the compound less potent in relation to cancer cells and more toxic in relation to normal cells indicating a loss of selectivity toward cancer cells. Similarly, either a decrease in anti-cancer activity and/or loss of tumor selectivity was observed when the extension of the 3-amino substituent in compound **1** was a phenethyl (compound **36**), a pyridine (compound **37**), a 1,3-thiazole (compound **38**) or a phenyl group with or without fluorine, chlorine, hydroxyl, and methyl groups at different positions (compounds **39–45**). We conclude that various extensions of the 3-amino group of 2-chloro-3-amino-1,4-NQ is detrimental to anti-cancer activity and selective cytotoxicity index. A lack of significant cancer cell specificity and reduced anti-cancer activity were also observed regardless of whether triazadien or 3,5-dimethylmorpholin was at the C-3 position (compounds **46** and **47**). The highest selective cytotoxicity index (>90) and low EC₅₀ (0.2 and 1.0 μM) in cancer cells were for compounds that have a 3-amino (compound **1**) and a 3-(2,3-dimethylaziridin-1-yl) (compound **16**) substituent, respectively. For comparison, a potent anti-cancer drug doxorubicin showed similar EC₅₀ in MIA PaCa-2 cells (0.2 μM), but its selective cytotoxicity index was approximately 25 times less (Fig 6).

According to our MS/MS analysis, NSC130362 efficiently reacts with GSH and most likely with any accessible sulfhydryl group present in a cysteine residue of proteins [7]. We believe that this reactivity is responsible for the short half-life of NSC130362 in the bloodstream. In the previous studies, we also showed that this reaction does not affect the ability of NSC130362 to inhibit GSR and cause oxidative stress. Based on this information, we selected the next set of 1,4-NQs that do not contain 2-chloro substituent (Fig 7).

We compared 1,4-NQs with 2-chloro-1,4-NQs that have identical C-3 position substituent to determine the role of the 2-chloro group in compound activity. Removal of the C-2 position chloro group in compounds **3**, **4**, **5**, and **12** to generate compounds **48**, **49**, **50**, **51**, and **52** reduced anti-cancer activities. When the C-3 position substituent was a primary amino group (compounds **1** and **48**), this chlorine removal increased toxicity to hepatocytes approximately 3-fold. In all other pairs, removal of the C-2 chloro group did not significantly affect toxicity to hepatocytes. We also noticed that with increasing the length of 3-alkylamino substituent, the effect of 2-chloro group on the anti-cancer activity was decreased. For example, when compounds have a 3-ethylamino substituent (compounds **3** and **49**), a 2-chlorine insertion was associated with a marked increase in cytotoxicity in MIA PaCa-2 cells, while the presence of a 3-propylamino (compounds **4** and **50**), 3-isobutylamino (compounds **12** and **52**), and 3-butylamino (compounds **5** and **51**) substituent gradually decreased the effect of the 2-position chloro group on anti-cancer activity.

On the other hand, exchange of the C-2 position chlorine in 2-chloro-3-(dimethylamino)-1,4-NQ (compound **14**) and 2-chloro-3-(aziridin-1-yl)-1,4-NQ (compound **15**) for a methoxy group to generate compounds **53** and **54**, respectively did not significantly affect the anti-cancer activity but greatly reduced toxicity to hepatocytes. Moreover, exchange of the C-2 position chlorine in compound **15** for a methyl group (compound **55**) increased the anti-cancer activity 2-fold and reduced toxicity to hepatocytes more than 10-fold. Again, we see the opposite effect of the substitution on the activity toward cancer and normal cells. Based on these data, we conclude that the C-2 position chlorine substituent (such as in NSC130362) was not necessary for

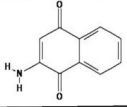
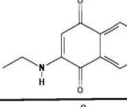
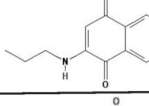
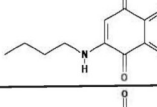
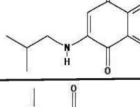
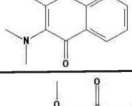
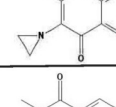
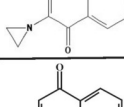
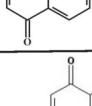
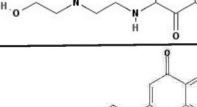
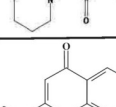
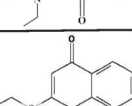
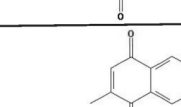
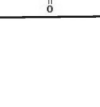
N	Name	Structure	EC50, μ M				Selective cytotoxicity index
			MIA PaCa-2		Hepatocytes		
				ATO		ATO	
48	NSC7936		24.4	1.0	28.1	6.9	6.9
49	NSC222687		>90.0	14.0	>90.0	>90.0	6.4
50	NSC409295		>90.0	22.2	>90.0	>90.0	4.1
51	NSC225988		>90.0	23.1	>90.0	>90.0	3.9
52	NSC225605		>90.0	24.3	>90.0	>90.0	3.7
53	NSC121721		23.4	1.9	>90.0	>90.0	47.4
54	NSC39051		7.5	0.9	>90.0	>90.0	100.0
55	NSC139346		3.1	0.6	>90.0	30.0	50.0
56	1,4-NQ		9.2	2.3	1.8	2.8	1.2
57	NSC299189		>90.0	11.2	83.2	>90.0	8.0
58	NSC35622		52.0	6.3	98.0	90.0	14.3
59	NSC222690		98.0	15.5	98.0	90.0	5.8
60	NSC148596		6.2	1.8	3.3	1.7	0.9
61	Menadione		7.8	1.5	11.8	15.6	10.4

Fig 7. EC50 values and the selective cytotoxicity index of the NSC130362 analogs that do not contain 2-chloro substituent in MIA PaCa-2 cells and hepatocytes. Standard deviation for all EC50 values does not exceed 10%. To calculate the selective cytotoxicity index for compounds that have the LC50 value above 90 μ M, EC50 values were equated to 90 μ M. $P < 0.05$.

<https://doi.org/10.1371/journal.pone.0205623.g007>

the anti-cancer activity and when a compound contains either the C-3 position dimethylamino (compound 53) or aziridin-1-yl (compound 54 and 55) substituent, it resembles NSC130362 in terms of anti-cancer activity and low level of toxicity to hepatocytes.

We also analyzed 1,4-NQs with or without C-3 position amino substituents. In comparing 1,4-NQ (compound 56) with 3-amino-1,4-NQ (compound 48) and 3-alkylamino-1,4-NQs (compounds 49–52), it was found that, in contrast to compounds 48–52, 1,4-NQ does not exhibit any tumor selectivity. Among compounds 48–52 and 56, 3-amino-1,4-NQ (compound 48) was the most active against cancer cells and its tumor selectivity was reflected by the selective cytotoxicity index equal to 6.9. In contrast to 1,4-NQ and 3-amino-1,4-NQ (compounds 56 and 48), all tested 3-alkylamino-1,4-NQs (compounds 49–52) were completely non-toxic to human hepatocytes ($EC_{50} > 90 \mu$ M). We conclude that the presence of 3-alkylamino substituent confers tumor selectivity. Similarly, insertion of a 2-(2-hydroxyethylamino)ethylamino, a 1-piperidinyl or a 2-diethylamino group at 3-position (compounds 57–59) increased EC_{50} in cancer cells compared to that of 1,4-NQ (compound 56), and eliminated any detectable toxicity to hepatocytes ($EC_{50} > 90 \mu$ M). In contrast, insertion of a C-3 position 2-hydroxyethylsulfanyl group (compound 60) resulted in slightly decreased EC_{50} in both cancer ($EC_{50} = 1.8 \mu$ M) and normal ($EC_{50} = 1.7 \mu$ M) cells. Another reference compound, menadione [30] (compound 61), which is 3-methyl-1,4-NQ, showed 1.5-fold improved anti-cancer activity as compared to 1,4-NQ (compound 56) and it was approximately 5 times less toxic to hepatocytes ($EC_{50} = 15.6 \mu$ M).

Finally, we analyzed quinoline-5,6-diones (Fig 8). When the naphthalene unit of the 1,4-NQ backbone of compound 1 (2-chloro-3-amino-1,4-NQ) was replaced with a quinoline, the resulting compound 62 almost completely lost tumor selectivity without losing anti-cancer activity. On the other hand, the same exchange of the 1,4-backbone in compound 14 and 48 to generate compound 63 and 64, respectively did not significantly affect either the anti-cancer activity or toxicity to hepatocytes, while the conversion of compound 49 into compound 66 improved the anti-cancer activity more than 30 times without affecting toxicity to hepatocytes. These data suggest that either the type of the 3-position substituent or the presence of the 2-chloro group in a 1,4-NQ derivative influences the effect of the naphthalene/quinoline exchange on either the anti-cancer activity or toxicity to hepatocytes. Furthermore, either complete removal of the C-2 position substituent or exchange of the 2-chloro group with bromine in compound 61 to generate compounds 64 or 65, reduced both the anti-cancer activity and toxicity to hepatocytes. We conclude that the 7-position substituent in quinoline-5,6-diones, which corresponds to the C-2 position substituent in 1,4-NQs, also contributes to the level of the anti-cancer activity and toxicity to hepatocytes. Interestingly, when the 6-position primary amino group of compound 64 was replaced by an anilino group, creating compound 67, a well-known GSR inhibitor LY83583, anti-cancer activity increased approximately 10-fold, while toxicity to hepatocytes was decreased 3-fold. It is noteworthy that the effect of the amine/aniline exchange in compound 64 to generate compound 66 is opposite to that of the amine/aniline exchange in compound 1, where the resulting compound 39 had 8-fold reduced anti-cancer activity and completely lost tumor selectivity. These data again suggest that careful selection of substituents in the quinone unit of either 1,4-NQs or quinoline-5,6-diones can result in improved anti-cancer activity and without negative effect on hepatocytes.

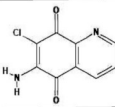
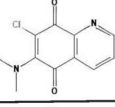
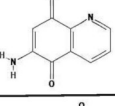
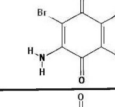
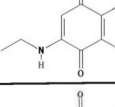
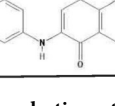
N	Name	Structure	EC50, μ M				Selective cytotoxicity index
			MIA PaCa-2		Hepatocytes		
				ATO		ATO	
48	NSC81056		1.5	0.2	4.6	0.3	1.5
49	NSC81046		8.9	2.0	8.0	8.0	4.0
50	NSC76886		20.8	1.9	12.4	6.5	3.4
51	NSC105808		1.8	0.4	8.6	4.1	10.3
52	NSC291094		4.5	0.4	>90.0	>90.0	225.0
53	LY83583		1.0	0.2	17.8	19.4	97.0

Fig 8. EC50 values and the selective cytotoxicity index of NSC130362 analogs in MIA PaCa-2 cells and hepatocytes. Standard deviation for all EC50 values does not exceed 10%. $P < 0.05$.

<https://doi.org/10.1371/journal.pone.0205623.g008>

Activities of the selected NSC130362 analogs

For further analyses, we used compounds that have the selective cytotoxicity index either above 20 (non-toxic compounds) or below 1 (toxic compounds) with the aim to identify targets that are responsible for the selective activity of the identified compounds toward cancer cells. To confirm that the effects of the selected compounds are not only specific to MIA PaCa-2 cells, we evaluated their cytotoxic activities on breast carcinoma HCC1187 cells (Table 1). HCC1187 cells were chosen because these cells are highly responsive to ROS [7]. For easy comparison, the data with MIA PaCa-2 cells were also included in Table 1. With only a few exceptions, all non-toxic compounds had a selective cytotoxicity index above 10 in HCC1187 cells. We also noticed that, again with a few exceptions, HCC1187 cells are more resistant to the non-toxic compounds in the presence of ATO as compared to MIA PaCa-2 cells. In contrast, HCC1187 cells are more sensitive to all toxic compounds in the presence of ATO as compared to MIA PaCa-2 cells. The high sensitivity of HCC1187 cells to toxic compounds contributed to the increased selective cytotoxicity index. In fact, all selected compounds had a selective cytotoxicity index above 1 for HCC1187 cells. Based on these results we conclude that despite the difference in sensitivity to some compounds, targeting both HCC1187 and MIA PaCa-2 cells by the non-toxic compounds most likely occurs *via* shared mechanisms.

The marked difference in the anti-tumor activity and selective cytotoxicity index between the non-toxic and toxic compounds (Table 1) indicates that these two groups of compounds should differ in either physicochemical properties or biological activities. Analysis of lipophilicity indicates that both the non-toxic and toxic compounds have similar distribution

Table 1. Activities of the selected NSC130362 analogs.

Name	LC50		LC50		LC50		LC50		Selective cytotoxicity index		ROS increase, %		Mito Check 1 ^a	GSR ^a	H ₂ O ₂ generation		GAPDH ^a	LogD, pH = 7.4
	HCC1187	MIA PaCa-2	Hepatocytes	Hepatocytes	HCC 1187	MIA PaCa-2	MIA PaCa-2	Hepato-cytes	MIA PaCa-2	ATO	ATO	MIA PaCa-2			-	+		
66 NSC291094	13.2	4.4	4.5	0.4	>90	>90	ATO	20.5	225.0	626	173	158	59	5.4	10.3	93	2.87	
54 NSC39051	18.2	2.2	7.5	0.9	>90	>90	ATO	40.9	100.0	675	124	84	54	2.4	3.9	73	0.31	
67 LY83583	3.0	0.2	1.0	0.2	17.8	19.4	97.0	8.7	95.5	783	179	116	53	5.5	11.9	76	3.45	
1 NSC3910	10.8	2.2	8.4	0.2	17.0	19.1	8.7	9.5	90.0	331	156	145	33	4.1	7.6	100	2.01	
16 NSC35852	3.6	0.7	6.9	1.0	78.0	>90	128.6	15.8	50.0	637	180	58	75	2.1	3.8	100	0.70	
55 NSC139346	51.8	1.9	3.1	0.6	>90	30.0	15.8	9.5	47.4	416	125	72	83	2.1	3.3	100	0.12	
53 NSC121721	>90	9.5	23.4	1.9	>90	>90	9.5	4.9	26.8	446	117	51	61	1.5	2.5	95	0.00	
17 NSC130362	19.2	1.5	9.8	1.8	83.0	70.0	46.7	38.9	295	295	132	38	65	2.6	4.8	89	1.12	
23 NSC91099	19.2	5.0	27.7	1.6	85.7	62.2	12.4	38.9	284	284	133	93	66	3.8	5.9	100	0.86	
13 NSC91107	28.7	1.5	7.2	1.0	29.9	26.8	17.9	26.8	248	248	123	84	45	2.7	4.3	100	0.52	
12 NSC91098	5.2	4.7	13.8	0.9	60.4	23.0	4.9	26.8	254	254	154	104	65	6.5	6.4	100	0.00	
3 NSC3860	23.6	4.4	59	2.9	81.9	74	16.8	25.5	182	182	115	93	59	3.9	6.3	100	1.01	
60 NSC148596	0.6	0.2	6.2	1.8	3.3	1.7	8.5	0.9	2188	2188	386	212	38	6.9	12.7	88	2.99	
40 NSC142581	9.0	5.1	78.5	21.3	24.5	19.6	3.8	0.9	111	111	122	103	72	5.0	2.9	88	0.00	
8 NSC91101	56.1	22.3	>90	62.8	78.6	54.6	2.4	0.9	110	110	115	116	93	2.0	2.8	100	0.17	
36 NSC41098	2.6	2.6	16.2	8.4	8.8	6.4	2.5	0.8	721	721	178	135	42	7.0	6.3	97	0.00	
39 NSC4285	1.7	0.4	3.9	1.6	2.3	1.2	3.0	0.8	1247	1247	174	91	92	1.6	2.8	93	0.13	
38 NSC337757	20.3	8.1	>90	>90	26.0	24.0	3.0	0.3	100	100	100	105	90	1.9	2.7	100	0.10	
26 NSC106715	1.7	0.7	26.6	13.7	4.8	3.6	5.1	0.3	889	889	191	112	66	5.9	3.8	94	0.00	
32 NSC130441	0.3	0.7	10.2	6.7	2.2	1.6	2.3	0.2	506	506	249	135	1	6.3	10.6	3	2.79	
31 NSC124994	1.0	0.5	10.4	5.9	1.6	1.3	2.6	0.2	251	251	228	159	28	5.7	9.0	5	2.03	

^a Enzyme residual activity after treatment as compared to DMSO-treated sample.

^b Concentration of H₂O₂ (μM) generated in the presence or absence of NADH/NADPH-dehydrogenase. *P* < 0.05.

<https://doi.org/10.1371/journal.pone.0205623.t001>

coefficient LogD that ranges from 0 to 3.45. We conclude that the analysis of the octanol-water partitioning is not sufficient to establish a link between degree of lipophilicity and biological activities of the selected compounds.

The cytotoxic effects of quinones have been attributed to several mechanisms: (i) DNA damage mediated *via* inhibition of DNA topoisomerase-II [31]; (ii) production of ROS *via* NADH/NADPH dehydrogenase-mediated formation of semiquinone radical that can reduce oxygen to produce super oxide [15]; (iii) inhibition of glyceraldehyde 3-phosphate dehydrogenase (GAPDH) [16], (iv) inhibition of GSR [7, 16, 32], (v) alkylation of cellular nucleophiles such as GSH, DNA, RNA and proteins, and (vi) inhibition of mitochondrial function [16, 21]. To elucidate the type of compound activity which is responsible for its cytotoxic effects in cancer cells and which is tolerated in normal cells, we performed various *in vitro* and cell-based activity assays (Table 1).

ROS induction in MIA Paca-2 cells and hepatocytes. As the first step, we evaluated the ability of the selected compounds to induce ROS in cancer and normal cells. Cells were incubated with the compounds for 4 h and the level of ROS induction was measured by a hydrogen peroxide cell-based assay kit. Compounds were assayed at a fixed concentration of 30 μ M and the measured level of hydrogen peroxide was expressed as percentage in relation to DMSO-treated cells (100%). As shown in Table 1, all non-toxic compounds induced more ROS in cancer cells than in hepatocytes. This distinction was more evident for compounds with the highest selective cytotoxicity index. Approximately half of the toxic compounds also induced more ROS in cancer cells than in normal cells. We conclude that the selective induction of ROS in cancer cells is required but not sufficient factor for the selective anti-tumor activity.

NADH/NADPH dehydrogenase-mediated redox cycling. As the next step, we examined the capability of the selected compounds to generate ROS in the presence or absence of NADH/NADPH dehydrogenase (Table 1). ROS can be generated by NADH/NADPH-dehydrogenase *via* the one electron reduction of a quinone ring of 1,4-NQs [15, 33]. Unstable half-reduced quinones (semiquinones) transfer electrons to molecular oxygen, thus generating superoxide anion radicals (O_2^-), which are converted by SOD to hydrogen peroxide [34]. We believe that our assay measuring compound's ability to generate H_2O_2 in the presence or absence of NADH/NADPH dehydrogenase more closely resembles conditions inside the cell than the assay designed to measure compound's redox potential values. In agreement with this hypothesis, it has been shown that rates of NADH/NADPH dehydrogenase-mediate quinone reduction do not correlate with the half-wave reduction potential values of quinones [33]. To determine the ability of compounds to induce ROS, compounds were incubated for 4 h at 37°C with and without NADH/NADPH-dehydrogenase in the presence of NADPH as an electron donor and SOD to convert generated superoxide radicals into hydrogen peroxide. At the end of incubation, 10-acetyl-3,7-dihydroxyphenoxazine (ADHP) and horseradish peroxidase (HRP) were added to the reaction and the level of HRP-mediated formation of the fluorogenic product, resorufin, was measured on a plate reader. ROS production was detected in reactions with either the toxic or non-toxic compounds. Surprisingly, we noticed that some toxic compounds generate more ROS in the absence of NADH/NADPH dehydrogenase than its presence. Based on these results, we conclude that the ability to generate ROS *via* NADH/NADPH-dehydrogenase mediated redox cycling cannot be the sole factor contributing to the selective anti-cancer activity of the tested compounds.

Effect on mitochondrial function. To further investigate the mechanism of anti-cancer activity, we evaluated the ability of the selected compounds to target mitochondria because inhibition of mitochondrial function by 1,4-NQs can be lethal to a cell [16]. Complex I consisting of NADH dehydrogenase constitutes one of the major sites of electron entry into the mitochondrial electron transport chain (ETC). Complex I catalyzes the transfer of two electrons from NADH to ubiquinone to form ubiquinol and finally to the terminal electron acceptor,

molecular oxygen. During this process, four protons are moved from mitochondria to the transmembrane space forming a pH gradient and an electrical potential across the inner mitochondrial membrane, which are required for oxidative phosphorylation. To test possible effects of compounds on ETC, we analyzed the Complex I-mediated NADH oxidation using a MitoCheck Complex I Activity Assay Kit. The level of NADH oxidation was measured by a decrease in absorbance at 340 nm and expressed as percentage of residual activity in relation to DMSO-treated mitochondria (Table 1). Addition of either non-toxic or toxic compounds to bovine heart mitochondria at a concentration of 30 μ M caused both inhibition and stimulation of NADH oxidation. We noticed that the set of the non-toxic compounds mostly consists of inhibitors of Complex I activity, while the set of the toxic compounds does not have any Complex I inhibitory activity, except compound **39** that inhibited mitochondrial function by 9%. It is noteworthy that because both Complex I and NADH/NADPH-dehydrogenase use NADH as a source of electrons, observed activity of Complex I does not correspond to the actual Complex I activity. Complex I activity was estimated by the rate of NADH oxidation which was also affected by NADH/NADPH-dehydrogenase-mediated redox cycling. Indeed, we noticed that compounds **1**, **31**, **32**, **36**, **60**, and **66** that stimulated Complex I Activity by more than 30% also induced a high level of ROS in the NADH/NADPH dehydrogenase-mediated reaction *in vitro*. Thus, increased activity of Complex I most likely was observed due to the increased NADH oxidation by NADH/NADPH-dehydrogenase. On the other hand, compounds that both inhibited Complex I and stimulated ROS production actually were more potent inhibitors than can be estimated by the level of Complex I inhibition, because they also promoted NADH oxidation by NADH/NADPH-dehydrogenase. Altogether, these data suggest that there was a bias of the non-toxic compounds to inhibitors of Complex I activity.

GSR Inhibition activity. Next, we evaluated the inhibitory activity of the selected compounds against human GSR enzyme using recombinant GSR and Abcam GSH/GSSG ratio detection reagent (Table 1). Briefly, GSR activity was measured by following oxidized glutathione (GSSG) reduction in the presence of NADPH and expressed as percentage of residual activity with respect to DMSO-treated enzyme. The residual activity of GSR for both the non-toxic and toxic compounds was quite heterogeneous, ranging from 100% (compounds **38**) to 3% (compound **32**). Remarkably, two compounds **31** and **32** with the lowest selective cytotoxicity index were the most potent inhibitors of GSR. We thus conclude that GSR inhibitory activity alone cannot be used to predict the selective cytotoxicity index.

GAPDH Inhibition Activity. As a final step, we evaluated the inhibitory activity of the selected compounds against human GAPDH enzyme in a cell-based assay using MIA PaCa-2 cells (Table 1). Cells were pre-incubated with compounds for 2 h at 37°C followed by cell lysis using sonication and GAPDH activity assay. The ability of compounds to inhibit GAPDH was expressed as percentage of GAPDH residual activity with respect to DMSO-treated cells. As shown in Table 1, most compounds inhibited GAPDH by 0 to 27%. Similar to the GSR activity assay, only two of the most toxic compounds **31** and **32**, were able to inhibit GAPDH by 95 and 97%, respectively. Based on these data, we conclude that inhibition of GAPDH is not the activity responsible for the selective cytotoxicity of the non-toxic compounds.

To evaluate if any nontoxic compounds' activities in the described cell-based and *in vitro* assays were significantly different from those of the toxic compounds, we calculated average activity values for each type of assay and determined the ratio between the nontoxic and toxic compounds (Fig 9). In addition, we performed a two-tailed t-test to determine if the difference in activities of the nontoxic and toxic compounds is significant or not. Our data showed that despite that the calculated ratios varied from 0.63 (ROS increase in MIA PaCa-2 cells) to 1.26 (GAPDH activity assay), only the effect of the nontoxic and toxic compounds on mitochondrial ETC is significantly different ($P = 0.029$) (Fig 9).

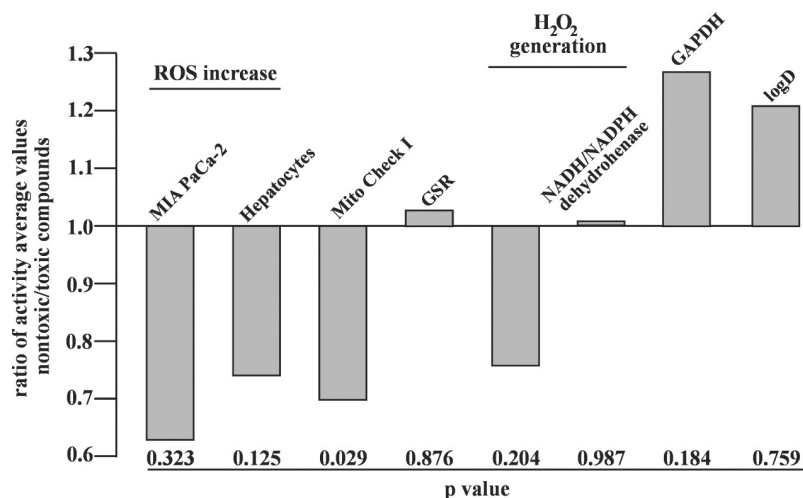


Fig 9. Activities of the nontoxic and toxic compounds. Ratio of activity average values between the nontoxic and toxic compounds in cell based and *in vitro* assays described in Table 1. P value for difference in activities of the nontoxic and toxic compounds in each type of assay is indicated below the corresponding bar.

<https://doi.org/10.1371/journal.pone.0205623.g009>

Quantitative SAR (QSAR) model

The mechanism of anti-tumor action of the non-toxic compounds should differ from that of the toxic compounds. Based on the obtained results we determined that except targeting mitochondrial ETC, the non-toxic compounds do not exhibit biological activities that are clearly distinct from those of toxic compounds. Since targeting mitochondria could involve different proteins and enzymes and chemical reactions of quinones are complex, we assumed that molecular modeling, which takes into account all available physicochemical properties of analyzed molecules, is an appropriate tool to identify key structural features that are associated with the observed selective cytotoxic activity. To accomplish this task, we employed the Q-MOL molecular modeling package (www.q-mol.com) [7, 35, 36] that uses a novel proprietary approach to take into account molecular flexibility, a common roadblock for many other molecular modeling tools. Taking into account the structure of the non-toxic and toxic compounds, Q-MOL developed a mathematical model or fitness function to distinguish accurately compounds with desired properties (anti-tumor activity and safety toward normal cells) (Fig 10). This fitness function was based on atom field potentials (AFPs) which, in turn, were

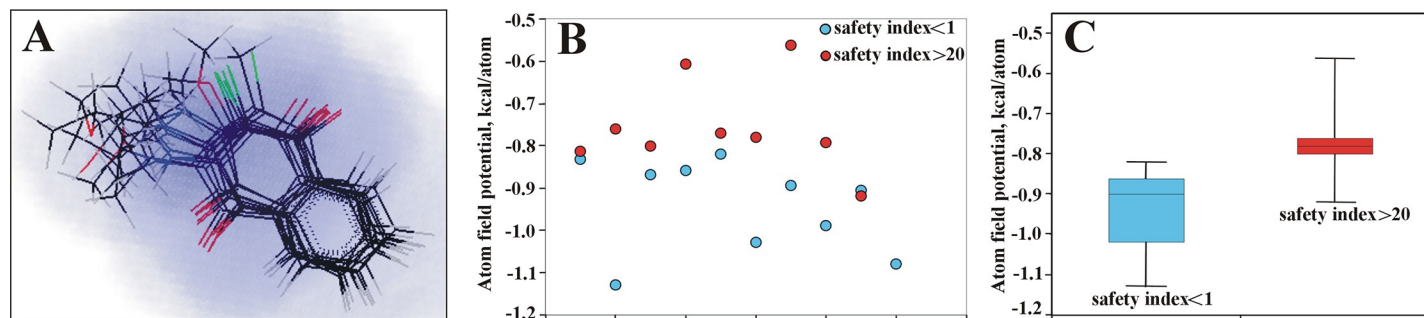


Fig 10. QSAR modeling of NSC130362 analogs. A. 3-D alignment of NSC130362 analogs. Red, blue and green color denote oxygen, nitrogen, and chlorine atoms, respectively; B, the distribution of the non-toxic (selective cytotoxicity index above 20) and toxic (selective cytotoxicity index below 1) analogs in relation to AFP; C, an average of AFPs for the nontoxic and toxic compounds. $P < 0.05$.

<https://doi.org/10.1371/journal.pone.0205623.g010>

derived from molecular mechanics force field. As shown in Fig 10, the resulting mathematical model shows that the non-toxic compounds have higher (less negative) AFPs than the toxic compounds.

Discussion

Recently, we published that NSC130362 inhibits GSR and, as a consequence, induces ROS and subsequent apoptosis in cancer cells but not in normal human hepatocytes as a model for hepatotoxicity [7]. Elevated ROS as compared to normal cells have been detected in almost all cancers. ROS promote tumor development and progression. To cope with the increased ROS, tumor cells also express increased levels of antioxidant proteins. A goal for ROS-based cancer therapy will be the ability to either target the antioxidant proteins that are used by tumor cells to detoxify from ROS or affect ROS producing pathways that result in increased ROS production. By achieving this goal, the ROS-based treatment could result in selective induction of apoptosis in cancer cells [1–7]. The aim of this study was two-fold: (1) to identify specific biological activities or structural features, which are responsible for the observed selective anti-cancer activity and (2) to determine whether a QSAR model could be designed for the development of potent anti-cancer compounds that are non-toxic toward normal cells. The NIH has defined several necessary conditions that should be met for validation of a compound to be target for optimization studies. Some of these conditions such as reproducible response in different assay types and adequate anti-tumor activity were addressed in our previous work [7]. To further validate NSC130362 as a candidate molecule for further characterization and/or development, we performed additional cell-based assays. ROS inducers and GSR inhibitors are also considered as drug sensitizers [22–24, 37]. Indeed, we showed that NSC130362 potentiated anti-tumor potency of all tested pancreatic and prostate cancer drugs and decreased EC50 (cytotoxicity) of several kinase inhibitors by up to 3-logs (1000 times) in leukemia cells directly *ex vivo* from patients. The ability to potentiate the cytotoxic activity of various anti-cancer agents is a valuable property of NSC130362. This conclusion is based on the fact that under treatment, cancer cells often adapt and develop resistance to anti-cancer drugs. To maximally exploit chemotherapy as a therapeutic strategy, it would be meaningful to combine anti-cancer agents with compounds that target these adaptive mechanisms. One of the mechanisms of adaptation that can confer chemoresistance is upregulation of antioxidant pathways. In agreement, there is accumulating evidence showing improved treatment outcome when anti-cancer drugs are combined with ROS-inducing agents [22–24]. In line with this evidence, our data also suggest that anti-cancer activity of the NSC130362/ATO combination is affected by the reducing environment inside cancer cells. It may be the case that targeting GSR activity, which controls the reducing environment in cancer cells, makes them susceptible to ATO and thus inducing apoptosis by altering redox-sensitive proteins and enzymes [27]. The reason that the effect of hypoxic conditions on the activity of the NSC130362/ATO combination is not pronounced is likely because ETC can function efficiently at oxygen levels as low as 0.5% [38]. However, we also noticed that NSC130362 had negative effect on the action of some compounds as seen in Fig 3A and Supporting Information S1 Table. We think that NSC130362 could have negative effect on the action of some compounds because these compounds could exert negative effect on cancer cells by their antioxidant activities [39]. Because NSC130362 induces ROS and subsequent oxidative stress, its action could counteract the action of antioxidants.

In addition, NSC130362 belongs to the class of 1,4-NQs that consists of important and widely distributed compounds with a variety of pharmacological properties. 1,4-NQs contain two ketone groups which have the ability to accept electrons and generate ROS *via* NADH/

NADPH dehydrogenase-mediated redox cycling mechanism [15, 33]. 1,4-NQs can also react with different biological targets. The NCI have identified the quinone moiety as an important pharmacophore element for anti-cancer drugs [40] because it possesses several tumor-selective activities such as anti-proliferative and anti-angiogenesis activity [41, 42], ability to induce oxidative stress, apoptosis and necrosis [43], ability to inhibit DNA replication [44], ability to suppress glycolysis and mitochondrial function [15], and ability to inhibit NF- κ B and STAT3 signaling [37, 45]. As a consequence, quinone moieties are present in many cancer drugs such as anthracyclines, daunorubicin, doxorubicin, and mitomycin [15].

To determine structural features of NSC130362, which are responsible for the selective anti-cancer activity, we performed SAR analysis of NSC130362 analogs. In the course of SAR studies, we focused on changes to the quinone moiety of NSC130362 because 1,4-NQ derivatives with various substitutions in C-2 and C-3 positions have been shown to exhibit potent anti-cancer properties [20, 46]. Because we were interested in identifying mechanisms underlying the selective anti-cancer cytotoxicity, the non-toxic compounds (selective cytotoxicity index above 20) and toxic compounds (selective cytotoxicity index below 1) were, therefore, selected for further experiments. Our studies support the following model: (1) One of the most important findings is that the C-2 chloro group of NSC130362 is dispensable for its activity and it can be removed to potentially improve pharmacokinetics (PK) and safety of the compound. The highly reactive C-2 chloro group may contribute to the short half-life of NSC130362 in the mouse bloodstream [7]. In addition, in agreement with our data, chlorine insertion at C-3 contributes to redox potential and reduced the selective cytotoxicity index, which was determined by comparing the IC₅₀ measured in cancer cells versus that obtained in normal fibroblasts [47]. These results are consistent with the chloro group at the C-2 position contributing to selectivity toward cancer cells. (2) The presence of the carbonyl group in the C-3 substitution group in all cases reduced the selective cytotoxicity index, indicating a loss of selectivity toward cancer cells. (3) Two most toxic analogs (MIA PaCa-2-related selective cytotoxicity index = 0.2) almost completely inhibited GAPDH. Previous papers described the involvement of GAPDH in growth and programmed cell death in hepatocytes suggesting a link between GAPDH and toxicity to hepatocytes [48, 49]. However, further analysis is needed to determine whether the GAPDH inhibitory activity is associated with toxicity in hepatocytes. The findings indicate a strong SAR among different 1,4-NQs and quinoline-5,8-diones and highlight the significance of functional groups as substituents in these compounds affecting their anti-cancer activity and selective cytotoxicity index.

1,4-NQ has limited solubility in aqueous solutions. Converting the naphthalene backbone of 1,4-NQ into a quinoline by introduction of a nitrogen atom at C-5 or at C-8 can increase aqueous solubility. However, introduction of a nitrogen atom at the C-5 or at C-8 of 1,4-NQ derivative menadione can increase the oxidant character of the molecule [32, 50]. To explore this modification, we compared compounds **1** vs **62**, **14** vs **63**, **48** vs **64**, and **49** vs **66**. While in the case of compounds **1** vs **62**, the introduction of quinoline resulted in 64-fold increase in toxicity to hepatocytes without any noticeable effect on anti-cancer activity, the same modification in either compound **14** or **48** did not significantly affect either anti-cancer activity or toxicity to hepatocytes. In contrast, conversion of 1,4-NQ backbone in compound **49** to generate compound **66** resulted in more than 30-fold improved anti-cancer activity without any visible effect on toxicity to hepatocytes. We conclude that the effect of naphthalene/quinoline exchange depends on the presence of the 2-chloro substituent and functional groups at the C-3 and, most likely, at other positions. More detailed analysis of different substitutions in the described or other positions of either naphthalene or quinolone backbones would require additional compounds be synthesized to make conclusive observations which is beyond the scope of this study.

With the aim of identifying the biological activity of the tested compounds that is responsible for the selective cytotoxicity in cancer cells, we tested the non-toxic (selective cytotoxicity index is above 20) and toxic (selective cytotoxicity index is below 1) compounds in a variety of cell-based and *in vitro* assays. In earlier studies it has been shown that the cytotoxic activity of 1,4-NQ is directly dependent on the redox potential, which accounts for the semiquinone production followed by autoxidation of semiquinone and generation of ROS [15, 20]. However, redox potentials of compounds cannot accurately predict their effects inside the cells because rates of NADH/NADPH dehydrogenase-mediate quinone reduction do not correlate with the half-wave reduction potential values of quinones [33]. For these reasons, we tested the selected compounds in cell-based assays as well as in direct *in vitro* ROS assays in the presence or absence of recombinant NADH/NADPH dehydrogenase to analyze the compound's ability to generate ROS. While all non-toxic compounds preferentially induce ROS in cancer cells, five out of nine toxic compounds also induced more ROS in cancer cells than in normal cells. In addition, the results of NADH/NADPH dehydrogenase-based *in vitro* assay confirmed that ROS-inducing capability cannot be the sole factor contributing to the value of the selective cytotoxicity index. Moreover, we noticed that three toxic compounds generated more ROS in the absence of NADH/NADPH dehydrogenase than when this enzyme was present in the reaction. We conclude that at least some toxic compounds induce ROS in cancer cells and hepatocytes by a mechanism that does not involve NADH/NADPH dehydrogenase.

To control the level of ROS and maintain redox homeostasis, mammalian cells have developed multiple strategies that inactivate ROS and prevent its accumulation. One such strategy is governed by the GSH/GSR-based electron donor system. Thus, compounds that target GSR can induce oxidative stress and subsequent cell death. To explore this possibility, we tested the selected compounds in *in vitro* GSR activity assays. All non-toxic compounds exhibited a moderate level of GSR-inhibiting activity ranging from 17% (compound 55) to 67% (compound 1), while the toxic compounds had much wider range from 7% (compound 8) to 99% (compound 32). We also noticed that the level of induced ROS in cancer cells does not necessarily correlate with the ability of compounds to produce ROS *in vitro* and inhibit GSR. This discrepancy can be explained by the different ability of compounds to penetrate cells where the compound's intracellular concentration could be 100–1000 times higher than its extracellular concentration as has been described for phenylethyl isothiocyanate (PEITC) [51, 52]. In addition, there are additional pathways that regulate ROS production and levels in cells that do not involve GSR. These could be manifest in intact cells.

The effect of 1,4-NQs on mitochondrial function [16] could play a major role in their activity and selectivity. Indeed, we found that most non-toxic compounds inhibited oxygen consumption supported by Complex I in bovine heart mitochondria. It is noteworthy that mitochondrial respiration was stimulated by the Complex I substrate NADH, which is also used as a donor of electrons in NADH/NADPH dehydrogenase-mediated reduction of 1,4-NQs. Mitochondrial function was measured by the rate of NADH oxidation. Thus, actual inhibition of mitochondrial function should be greater than that we measured because of these two simultaneous reactions: Complex I and NADH/NADPH dehydrogenase. Indeed, the non-toxic compounds that showed induction of mitochondrial function (compounds 1, 66, and 67) had the highest ability to generate ROS in NADH/NADPH dehydrogenase-mediated reaction.

In contrast, all toxic compounds with one exception (compound 39 with 9% inhibition) did not inhibit mitochondrial respiration. Again, toxic compounds 31, 32, 36, and 60 with the highest ROS-inducing ability showed increased NADH oxidation in the Complex I activity assay. Based on these data, we conclude that effects on mitochondrial respiration could contribute to the selective anti-cancer activity of the non-toxic compounds. Indeed, we

determined that the ability of the nontoxic compounds to inhibit oxygen consumption by Complex I in bovine heart mitochondria is the only activity among tested that is significantly different from that of the toxic compounds. On the other hand, the toxic compounds induced cytotoxicity by mechanisms that are distinct from inhibition of mitochondrial respiration.

The mitochondria play a critical role in the production of ATP and the metabolites that are necessary for biosynthesis of macromolecules such as nucleotides, fatty acids, and glutathione [53]. The generation of ATP occurs *via* a set of mitochondrial intermembrane complexes I, III, and IV that make up the ETC. Recent studies provided evidence that the mitochondrial ETC might be a valuable target for cancer therapy [53, 54]. For example, it has been shown that metformin exerts anti-tumor effects partially through its ability to inhibit mitochondrial complex I and exhibits an excellent safety profile [53, 55]. Another inhibitor of complex I activity, phenformin, also exerts its anti-tumor effects in orthotopic mouse models [56]. It is noteworthy that, like NSC130362, inhibitors of mitochondrial function, including metformin and phenformin, improve the anti-cancer effects of compounds that target PI3K and B-RAF signaling [57–59]. Mitochondrial complex I inhibitors block tricarboxylic acid (TCA) cycle-mediated ATP production and induce apoptosis by enhancing the generation of ROS. A ROS-based approach to induce selective cytotoxicity in cancer cells has been recently validated by researchers at Kolkata's Indian Association for the Cultivation of Science (IACS) who have synthesized a novel porphyrin compound with potent anti-cancer activity [60]. By targeting cellular topoisomerase 1 enzyme and producing increased ROS inside cells, this porphyrin compound showed potent cytotoxicity against cervical, ovarian, and colon cancer cells with significantly reduced or no toxicity toward human embryonic kidney cell lines and mouse embryonic fibroblasts.

Although most cancer cells have functional mitochondrial metabolism, some cancer cells have mutations in the ETC and macromolecule biosynthesis proteins of their mitochondria [61, 62]. These cancer cells are dependent on glycolysis to produce energy (Warburg effect). Thus, inhibiting glycolysis is an efficient way to target these ETC-mutated cancer cells. In addition, one of the key hallmarks of cancer is to re-program metabolic capability, which leads to elevated glycolytic metabolism in cancer cell [63]. Thus, it has been hypothesized that inhibition of both mitochondrial metabolism and glycolysis could be an effective anti-cancer therapy [64]. GAPDH catalyzes the conversion of glyceraldehyde 3-phosphate to D-glycerate 1,3-bisphosphate in the process of glycolysis [65]. Because GAPDH is one of the possible targets of 1,4-NQ, we evaluated the selected compounds in cell-based GAPDH inhibition assays. None of the non-toxic compounds inhibited GAPDH by more than 27%. In contrast, two the most toxic compounds (compounds 31 and 32) almost completely inhibited GAPDH. Because the same compounds were the most efficient inhibitors of GSR, we speculated that this dual effect can be responsible for the high level of toxicity to hepatocytes and, as a consequence, the lowest selective cytotoxicity index of compounds 31 and 32. Other toxic compounds inhibited GAPDH with narrow range of 0–12%. We conclude that targeting glycolysis is not the factor that is responsible of the selective anti-cancer activity of the non-toxic compounds.

The results described above allow us to predict that targeting mitochondrial ETC could be the key biological activity that can be used to guide non-toxic compound optimization. We can also speculate that distinct effects of the non-toxic and toxic compounds on mitochondrial function are governed by multiple structural factors that include but are not limited to electronic, hydrophobic, and steric characteristics of substituents and their position in the quinone ring [66, 67]. To account for available physico-chemical factors that most likely affect compound activities, we performed molecular modeling to develop a QSAR model. Molecular modeling employed computational-based descriptors to correlate biological activity in cellular systems. Based on the structure of the non-toxic and toxic compounds, Q-MOL developed a

fitness function (AFPs) to describe accurately the relationship between the molecular structure of a chemical and its anti-tumor potency and safety toward normal cells. Encouragingly, there was a clear difference in the AFPs between the non-toxic and toxic compounds, which confirmed that the AFP-based QSAR model could be trained by docking ligands into AFP distributions and then used as an energy-based classifier to differentiate between non-toxic and toxic ligands. Thus, we concluded that obtained QSAR model can be used to design non-toxic compounds with potent anti-tumor activity. Overall, the obtained results improve our knowledge regarding mechanisms of the selective anti-cancer activity.

Supporting information

S1 Table. Combined treatment of kinase inhibitors with NSC130362 (10 μ M) against leukemia cells from patients.
(XLSX)

Author Contributions

Conceptualization: Gordon B. Mills.

Data curation: Cristina E. Tognon.

Formal analysis: Dmitri Rozanov, Anton Cheltsov, Aaron Nilsen, Gordon B. Mills, Paul Spellman.

Investigation: Dmitri Rozanov, Anton Cheltsov, Jeffrey Tyner.

Methodology: Dmitri Rozanov, Isaac Forquer, James Korkola, Jeffrey Tyner.

Resources: James Korkola, Joe Gray, Jeffrey Tyner, Cristina E. Tognon, Paul Spellman.

Supervision: Joe Gray, Gordon B. Mills, Paul Spellman.

Validation: Isaac Forquer.

Writing – original draft: Dmitri Rozanov.

Writing – review & editing: Christopher Boniface, Gordon B. Mills.

References

1. Sosa V, Moliné T, Somoza R, Paciucci R, Kondoh H, LLeonart ME. Oxidative stress and cancer: an overview. *Ageing Res Rev.* 2013; 12: 376–390. <https://doi.org/10.1016/j.arr.2012.10.004> PMID: 23123177
2. Reuter S, Gupta SC, Chaturvedi MM, Aggarwal BB. Oxidative stress, inflammation, and cancer: how are they linked? *Free Radic Biol Med.* 2010; 49: 1603–1616. <https://doi.org/10.1016/j.freeradbiomed.2010.09.006> PMID: 20840865
3. Pervaiz S, Clement MV. Tumor intracellular redox status and drug resistance—serendipity or a causal relationship? *Curr Pharm Des.* 2004; 10: 1969–1977. PMID: 15180532
4. Trachootham D, Zhou Y, Zhang H, Demizu Y, Chen Z, Pelicano H, et al. Selective killing of oncogenically transformed cells through a ROS-mediated mechanism by beta-phenylethyl isothiocyanate. *Cancer Cell.* 2006; 10: 241–252. <https://doi.org/10.1016/j.ccr.2006.08.009> PMID: 16959615
5. Zhang R, Humphreys I, Sahu RP, Shi Y, Srivastava SK. *In vitro* and *in vivo* induction of apoptosis by capsaicin in pancreatic cancer cells is mediated through ROS generation and mitochondrial death pathway. *Apoptosis.* 2008; 13: 1465–1478. <https://doi.org/10.1007/s10495-008-0278-6> PMID: 19002586
6. Pelicano H, Carney D, Huang P. ROS stress in cancer cells and therapeutic implications. *Drug Resist Updat.* 2004; 7: 97–110. <https://doi.org/10.1016/j.drug.2004.01.004> PMID: 15158766
7. Rozanov D, Cheltsov A, Sergienko E, Vasile S, Golubkov V, Aleshin AE, et al. TRAIL-based high throughput screening reveals a link between TRAIL-mediated apoptosis and glutathione reductase, a

- key component of oxidative stress response. PLoS One. 2015; 10: e0129566. <https://doi.org/10.1371/journal.pone.0129566> PMID: 26075913
8. Couzin J. Cancer drugs. Smart weapons prove tough to design. Science 2002; 298: 522–525. <https://doi.org/10.1126/science.298.5593.522> PMID: 12386312
 9. Frantz S. Drug discovery: playing dirty. Nature. 2005; 437: 942–943. <https://doi.org/10.1038/437942a> PMID: 16222266
 10. Lu J, Holmgren A. Thioredoxin system in cell death progression. Antioxid Redox Signal. 2012; 17: 1738–1747. <https://doi.org/10.1089/ars.2012.4650> PMID: 22530689
 11. Couto N, Wood J, Barber J. The role of glutathione reductase and related enzymes on cellular redox homeostasis network. Free Radic Biol Med. 2016; 95: 27–42. <https://doi.org/10.1016/j.freeradbiomed.2016.02.028> PMID: 26923386
 12. Kamada K, Goto S, Okunaga T, Ihara Y, Tsuji K, Kawai Y, et al. Nuclear glutathione S-transferase pi prevents apoptosis by reducing the oxidative stress-induced formation of exocyclic DNA products. Free Radic Biol Med. 2004; 37: 1875–1884. <https://doi.org/10.1016/j.freeradbiomed.2004.09.002> PMID: 15528046
 13. Fernando MR, Lechner JM, Löfgren S, Gladyshev VN, Lou MF. Mitochondrial thioltransferase (glutaredoxin 2) has GSH-dependent and thioredoxin reductase-dependent peroxidase activities *in vitro* and in lens epithelial cells. FASEB J. 2006; 20: 2645–2647. <https://doi.org/10.1096/fj.06-5919fje> PMID: 17065220
 14. Geisbrecht BV, Gould SJ. The human PICD gene encodes a cytoplasmic and peroxisomal NADP (+)-dependent isocitrate dehydrogenase. J Biol Chem. 1999; 274: 30527–33053. PMID: 10521434
 15. O'Brien PJ. Molecular mechanisms of quinone cytotoxicity. Chem Biol Interact. 1991; 80: 1–41. PMID: 1913977
 16. Prati F, Bergamini C, Molina MT, Falchi F, Cavalli A, Kaiser M, et al. 2-Phenoxy-1,4-naphthoquinones: From a Multitarget Antitrypanosomal to a Potential Antitumor Profile. J Med Chem. 2015; 58: 6422–6434. <https://doi.org/10.1021/acs.jmedchem.5b00748> PMID: 26237241
 17. Yan C, Siegel D, Newsome J, Chilloux A, Moody CJ, Ross D. Antitumor indolequinones induced apoptosis in human pancreatic cancer cells via inhibition of thioredoxin reductase and activation of redox signaling. Mol Pharmacol. 2012; 81: 401–410. <https://doi.org/10.1124/mol.111.076091> PMID: 22147753
 18. Nordhoff A, Bücheler US, Werner D, Schirmer RH. Folding of the four domains and dimerization are impaired by the Gly446→Glu exchange in human glutathione reductase. Implications for the design of antiparasitic drugs. Biochemistry. 1993; 32: 4060–4066. PMID: 8097111
 19. Hughes JP, Rees S, Kalindjian SB, Philpott KL. Principles of early drug discovery. Br J Pharmacol. 2011; 162: 1239–1249. <https://doi.org/10.1111/j.1476-5381.2010.01127.x> PMID: 21091654
 20. Prachayasittikul V, Pingaew R, Worachartcheewan A, Nantasenamat C, Prachayasittikul S, Ruchirawat S, et al. Synthesis, anticancer activity and QSAR study of 1,4-naphthoquinone derivatives. Eur Med Chem. 2014; 84: 247–263.
 21. Nicotera P, Hinds TR, Nelson SD, Vincenzi EF. Differential effects of arylating and oxidizing analogs of N-acetyl-p-benzoquinoneimine on red blood cell membrane proteins. Arch. Biochem. Biophys. 1990; 283: 200–205. PMID: 2146923
 22. Maiti AK. Genetic determinants of oxidative stress-mediated sensitization of drug-resistant cancer cells. International Journal of Cancer. 2012; 130: 1–9. <https://doi.org/10.1002/ijc.26306> PMID: 21792891
 23. Donadelli M, Costanzo C, Beghelli S, Scupoli MT, Dandrea M, Bonora A, et al. Synergistic inhibition of pancreatic adenocarcinoma cell growth by trichostatin A and gemcitabine. Biochimica et Biophysica Acta. 2007; 1773: 1095–1106. <https://doi.org/10.1016/j.bbamcr.2007.05.002> PMID: 17555830
 24. Maeda H, Hori S, Ohizumi H, Segawa T, Kakehi Y, Ogawa O, et al. Effective treatment of advanced solid tumors by the combination of arsenic trioxide and L-buthionine-sulfoximine. Cell Death and Differentiation. 2004; 11: 737–746. <https://doi.org/10.1038/sj.cdd.4401389> PMID: 15002036
 25. Hidalgo M. Pancreatic Cancer. N Engl J Med. 2010; 362: 1605–1617. <https://doi.org/10.1056/NEJMra0901557> PMID: 20427809
 26. Tyner JW, Yang WF, Bankhead A 3rd, Fan G, Fletcher LB, Bryant J, et al. Kinase pathway dependence in primary human leukemias determined by rapid inhibitor screening. Cancer Res. 2013; 73: 285–296. <https://doi.org/10.1158/0008-5472.CAN-12-1906> PMID: 23087056
 27. Miller WH Jr, Schipper HM, Lee JS, Singer J, Waxman S. Mechanisms of action of arsenic trioxide. Cancer Res. 2002; 62: 3893–3903. PMID: 12124315
 28. Ramadori G, Cameron S. Effects of systemic chemotherapy on the liver. Ann Hepatol. 2010; 9: 133–143. PMID: 20526005

29. Zhou S, Palmeira CM, Wallace KB. Doxorubicin-induced persistent oxidative stress to cardiac myocytes. *Toxicol Lett.* 2001; 121: 151–157. PMID: [11369469](#)
30. Criddle DN, Gillies S, Baumgartner-Wilson HK, Jaffar M, Chinje EC, Passmore S, et al. Menadione-induced reactive oxygen species generation *via* redox cycling promotes apoptosis of murine pancreatic acinar cells. *J Biol Chem.* 2006; 281: 40485–40492. <https://doi.org/10.1074/jbc.M607704200> PMID: [17088248](#)
31. Bender RP, Ham AJ, Osheroff N. Quinone-induced enhancement of DNA cleavage by human topoisomerase II α : adduction of cysteine residues 392 and 405. *Biochemistry.* 2007; 46: 2856–2864. <https://doi.org/10.1021/bi0620171> PMID: [17298034](#)
32. Morin C, Besset T, Moutet JC, Fayolle M, Brückner M, Limosin D, et al. The aza-analogues of 1,4-naphthoquinones are potent substrates and inhibitors of plasmodial thioredoxin and glutathione reductases and of human erythrocyte glutathione reductase. *Org Biomol Chem.* 2008; 6: 2731–2742. <https://doi.org/10.1039/b802649c> PMID: [18633531](#)
33. Buffinton GD, Ollinger K, Brunmark A, Cadenas E. DT-diaphorase-catalysed reduction of 1,4-naphthoquinone derivatives and glutathionyl-quinone conjugates. Effect of substituents on autoxidation rates. *Biochem J.* 1989; 257: 561–571. PMID: [2494985](#)
34. McCord JM, Fridovich I. Superoxide dismutase: the first twenty years (1968–1988). *Free Radic Biol Med.* 1988; 5: 363–369. PMID: [2855736](#)
35. Chen F, Chen J, Lin J, Cheltsov AV, Xu L, Chen Y, et al. NSC-640358 acts as RXR α ligand to promote TNF α -mediated apoptosis of cancer cell. *Protein Cell.* 2015; 6: 654–666. <https://doi.org/10.1007/s13238-015-0178-9> PMID: [26156677](#)
36. Shiryayev SA, Cheltsov AV, Gawlik K, Ratnikov BI, Strongin AY. Virtual ligand screening of the National Cancer Institute (NCI) compound library leads to the allosteric inhibitory scaffolds of the West Nile Virus NS3 proteinase. *Assay Drug Dev Technol.* 2011; 9: 69–78. <https://doi.org/10.1089/adt.2010.0309> PMID: [21050032](#)
37. Sandur SK, Ichikawa H, Sethi G, Ahn KS, Aggarwal BB. Plumbagin (5-hydroxy-2-methyl-1,4-naphthoquinone) suppresses NF- κ B activation and NF- κ B-regulated gene products through modulation of p65 and I κ B kinase activation, leading to potentiation of apoptosis induced by cytokine and chemotherapeutic agents. *J Biol Chem.* 2006; 281: 17023–17033. <https://doi.org/10.1074/jbc.M601595200> PMID: [16624823](#)
38. Rumsey WL, Schlosser C, Nuutinen EM, Robiolio M, Wilson DF. Cellular energetics and the oxygen dependence of respiration in cardiac myocytes isolated from adult rat. *J Biol Chem.* 1990; 265: 15392–15402. PMID: [2394731](#)
39. Saso L, Firuzi O. Pharmacological applications of antioxidants: lights and shadows. *Curr Drug Targets.* 2014; 15: 1177–1199. PMID: [25341421](#)
40. Liu KC, Li J, Sakya S. Synthetic approaches to the 2003 new drugs. *Mini-Rev Med Chem.* 2004; 4: 1105–1125. PMID: [15579116](#)
41. Hafeez BB, Zhong W, Fischer JW, Mustafa A, Shi X, Meske L, et al. Plumbagin, a medicinal plant (*Plumbago zeylanica*)-derived 1,4-naphthoquinone, inhibits growth and metastasis of human prostate cancer PC-3M-luciferase cells in an orthotopic xenograft mouse model. *Mol Oncol.* 2013; 7: 428–439. <https://doi.org/10.1016/j.molonc.2012.12.001> PMID: [23273564](#)
42. Kayashima T, Mori M, Yoshida H, Mizushima Y, Matsubara K. 1,4-Naphthoquinone is a potent inhibitor of human cancer cell growth and angiogenesis. *Cancer Lett.* 2009; 278: 34–40. <https://doi.org/10.1016/j.canlet.2008.12.020> PMID: [19168278](#)
43. Han W, Li L, Qiu S, Lu Q, Pan Q, Gu Y, et al. Shikonin circumvents cancer drug resistance by induction of a necroptotic death. *Mol Cancer Ther.* 2007; 6: 1641–1649. <https://doi.org/10.1158/1535-7163.MCT-06-0511> PMID: [17513612](#)
44. Shahabuddin MS, Gopal M. Genotoxicity of DNA Intercalating Anticancer Drugs: Pyrimido[4(1),5(1):4,5]thieno(2,3-b)quinolines on Somatic and Germinal Cells. *Toxicol Mech Methods.* 2007; 17: 135–145. <https://doi.org/10.1080/15376510600899605> PMID: [20020962](#)
45. Bhasin D, Etter JP, Chettiar SN, Mok M, Li PK. Antiproliferative activities and SAR studies of substituted anthraquinones and 1,4-naphthoquinones. *Bioorg Med Chem Lett.* 2013; 23: 6864–2867. <https://doi.org/10.1016/j.bmcl.2013.09.098> PMID: [24176397](#)
46. Sunassee SN, Veale CG, Shunmoogam-Gounden N, Osoniyi O, Hendricks DT, Cairra MR, et al. Cytotoxicity of lapachol, β -lapachone and related synthetic 1,4-naphthoquinones against oesophageal cancer cells. *Eur J Med Chem.* 2013; 62: 98–110. <https://doi.org/10.1016/j.ejmech.2012.12.048> PMID: [23353747](#)
47. Benites J, Valderrama JA, Bettega K, Pedrosa RC, Calderon PB, Verrax J. Biological evaluation of donor-acceptor aminonaphthoquinones as antitumor agents. *Eur J Med Chem.* 45 2010; 45: 6052–6057. <https://doi.org/10.1016/j.ejmech.2010.10.006> PMID: [20980080](#)

48. Barbini L, Rodríguez J, Dominguez F, Vega F. Glyceraldehyde-3-phosphate dehydrogenase exerts different biologic activities in apoptotic and proliferating hepatocytes according to its subcellular localization. *Mol Cell Biochem.* 2007; 300: 19–28. <https://doi.org/10.1007/s11010-006-9341-1> PMID: 17426931
49. Ciriaci N, Vigo B, Rigalli J, Mottino A, Ruiz M, Ghanem C. Acetaminophen (APAP) hepatocyte toxicity is associated with increased translocation of glyceraldehyde-3-phosphate dehydrogenase (GAPDH) to the nucleus. *FASEB J.* 2015; 29: Suppl 937.8.
50. Shaikh IA, Johnson F, Grollman AP. Streptonigrin. 1. Structure-activity relationships among simple bicyclic analogues. Rate dependence of DNA degradation on quinone reduction potential. *J Med Chem.* 1986; 29: 1329–40. PMID: 3525839
51. Xu K, Thornalley PJ. Involvement of glutathione metabolism in the cytotoxicity of the phenethyl isothiocyanate and its cysteine conjugate to human leukaemia cells in vitro. *Biochem Pharmacol.* 2001; 61: 165–177. PMID: 11163331
52. Trachootham D, Zhou Y, Zhang H, Demizu Y, Chen Z, Pelicano H, et al. Selective killing of oncogenically transformed cells through a ROS-mediated mechanism by beta-phenylethyl isothiocyanate. *Cancer Cell.* 2006; 10: 241–252. <https://doi.org/10.1016/j.ccr.2006.08.009> PMID: 16959615
53. Weinberg SE, Chandel NS. Targeting mitochondria metabolism for cancer therapy. *Nat Chem Biol.* 2015; 11: 9–15. <https://doi.org/10.1038/nchembio.1712> PMID: 25517383
54. Kalyanaraman B, Cheng G, Hardy M, Ouari O, Lopez M, Joseph J, et al. A review of the basics of mitochondrial bioenergetics, metabolism, and related signaling pathways in cancer cells: Therapeutic targeting of tumor mitochondria with lipophilic cationic compounds. *Redox Biol.* 2018; 14: 316–327. <https://doi.org/10.1016/j.redox.2017.09.020> PMID: 29017115
55. Janzer A, German NJ, Gonzalez-Herrera KN, Asara JM, Haigis MC, Struhl K. Metformin and phenformin deplete tricarboxylic acid cycle and glycolytic intermediates during cell transformation and NTPs in cancer stem cells. *Proc Natl Acad Sci U S A.* 2014; 111: 10574–10579. <https://doi.org/10.1073/pnas.1409844111> PMID: 25002509
56. Jackson AL, Sun W, Kilgore J, Guo H, Fang Z, Yin Y, et al. Phenformin has anti-tumorigenic effects in human ovarian cancer cells and in an orthotopic mouse model of serous ovarian cancer. *Oncotarget.* 2017; 8: 100113–100127. <https://doi.org/10.18632/oncotarget.22012> PMID: 29245964
57. Engelman JA, Chen L, Tan X, Crosby K, Guimaraes AR, Upadhyay R, et al. Effective use of PI3K and MEK inhibitors to treat mutant Kras G12D and PIK3CA H1047R murine lung cancers. *Nat Med.* 2008; 14: 1351–1356. <https://doi.org/10.1038/nm.1890> PMID: 19029981
58. Yuan P, Ito K, Perez-Lorenzo R, Del Guzzo C, Lee JH, Shen CH, et al. Phenformin enhances the therapeutic benefit of BRAF(V600E) inhibition in melanoma. *Proc Natl Acad Sci U S A.* 2013; 110: 18226–18231. <https://doi.org/10.1073/pnas.1317577110> PMID: 24145418
59. Zheng Z, Zhu W, Yang B, Chai R, Liu T, Li F, et al. The co-treatment of metformin with flavone synergistically induces apoptosis through inhibition of PI3K/AKT pathway in breast cancer cells. *Oncol Lett.* 2018; 15: 5952–5958. <https://doi.org/10.3892/ol.2018.7999> PMID: 29552226
60. Das SK, Ghosh A, Paul Chowdhuri S, Halder N, Rehman I, Sengupta S, et al. Neutral Porphyrin Derivative Exerts Anticancer Activity by Targeting Cellular Topoisomerase I (Top1) and Promotes Apoptotic Cell Death without Stabilizing Top1-DNA Cleavage Complexes. *J Med Chem.* 2018; 61: 804–817. <https://doi.org/10.1021/acs.jmedchem.7b01297> PMID: 29290109
61. Yang M, Soga T, Pollard PJ. Oncometabolites: linking altered metabolism with cancer. *J Clin Invest.* 2013; 123: 3652–3658. <https://doi.org/10.1172/JCI67228> PMID: 23999438
62. Wallace DC. A mitochondrial paradigm of metabolic and degenerative diseases, aging, and cancer: a dawn for evolutionary medicine. *Annu Rev Genet.* 2005; 39: 359–407. <https://doi.org/10.1146/annurev.genet.39.110304.095751> PMID: 16285865
63. Ward PS, Thompson CB. Metabolic reprogramming: a cancer hallmark even warburg did not anticipate. *Cancer Cell.* 2012; 21: 297–308. <https://doi.org/10.1016/j.ccr.2012.02.014> PMID: 22439925
64. Cheng G, Zielonka J, Dranka BP, McAllister D, Mackinnon AC Jr, Joseph J, et al. Mitochondria-targeted drugs synergize with 2-deoxyglucose to trigger breast cancer cell death. *Cancer Res.* 2012; 72: 2634–2644. <https://doi.org/10.1158/0008-5472.CAN-11-3928> PMID: 22431711
65. Ramzan R, Weber P, Linne U, Vogt S. GAPDH: the missing link between glycolysis and mitochondrial oxidative phosphorylation? *Biochem Soc Trans.* 2013; 41: 1294–1297. <https://doi.org/10.1042/BST20130067> PMID: 24059522
66. Buffinton GD, Ollinger K, Brunmark A, Cadenas E. DT-diaphorase-catalysed reduction of 1,4-naphthoquinone derivatives and glutathionyl-quinone conjugates. Effect of substituents on autoxidation rates. *Biochem J.* 1989; 257: 561–571. PMID: 2494985
67. Song Y, Buettner GR. Thermodynamic and kinetic considerations for the reaction of semiquinone radicals to form superoxide and hydrogen peroxide. *Free Radic Biol Med.* 2010; 49: 919–962. <https://doi.org/10.1016/j.freeradbiomed.2010.05.009> PMID: 20493944